

Quasiclassical theory of superconductivity: a multiple interface geometry

A. Shelankov* and M. Ozana

Department of Theoretical Physics, Umeå University, 901 87 Umeå, Sweden

Abstract

A new method which allows one to study multiple coherent reflection/transmissions by partially transparent interfaces, (e.g., in multi-layer mesoscopic structures or grain boundaries in high-T_c's), in the framework of the quasiclassical theory of superconductivity is suggested. It is argued that in the presence of interfaces, a straight-line trajectory transforms to a simple connected 1-dimensional tree (graph) with knots, i.e. the points where the interface scattering events occur and pieces of the trajectories are coupled. For the 2-component trajectory "wave function" which factorizes the Gor'kov matrix Green's function, a linear boundary condition on the knot is formulated for an arbitrary interface, specular or diffusive (in the many channel model). From the new boundary condition, we derive: (i) the excitation scattering amplitude for the multi-channel Andreev/ordinary reflection/transmission processes; (ii) the boundary conditions for the Riccati equation; (iii) the transfer matrix which couples the trajectory Green's function before and after the interface scattering. To show the usage of the method, the cases of a film separated from a bulk superconductor by a partially transparent interface, and a SIS' sandwich with finite thickness layers, are considered. The electric current response to the vector potential (the superfluid density ρ_s) with the π phase difference in S and S' is calculated for the sandwich. It is shown that the model is very sensitive to imperfection of the SS' interface: the low temperature response being paramagnetic ($\rho_s < 0$) in the ideal system case, changes its sign and becomes diamagnetic ($\rho_s > 0$) when the probability of reflection is as low as a few percent.

PACS numbers: 74.20.Fg, 74.50.+r, 74.80.D, 74.80F

I. INTRODUCTION

Many important properties of superconductors are related to surfaces and interfaces, the Josephson and proximity effects being well-known examples. In recent years, new rich surface physics has been found in high- T_c oxides after the identification of the d-symmetry of the order parameter. On the theoretical side, studying an interface poses certain problems: The method of the quasiclassical Green's functions [1–4] (for a recent review see [5])which is the main tool in the superconductivity theory, cannot be directly applied here since the quasiclassical condition is violated by fast change of the potentials on the atomic distances in the vicinity of the interface. As shown by Zaitsev [6], the abrupt changes at a specular partially transparent interface can be incorporated into a boundary condition for the quasiclassical Green's functions; the condition is a third order equation for the matrix Green's function near the interface. Various forms of the boundary condition have been discussed in more recent papers [7–9]. New difficulties arise when one attempts to describe the coherent reflection/transmission by many interfaces, e.g. in a multi-layer mesoscopic structures or grain boundaries network in high- T_c 's . In this case, Zaitsev's third order boundary condition must be satisfied on each interface, and one encounters the problem of solving a system of cubic matrix equations. It is not obvious that a solution to the system of equations exists and is unique if it exists. Moreover, some authors [7,8] doubt the very applicability of the quasiclassical scheme in the many interface geometry: They argue that the quasiclassical normalization, which is a vital part of the quasiclassical scheme, is not possible in a double layer system with partially reflective interface.

The purpose of the present paper is to re-examine the theory of the interface in the quasiclassical description of superconductivity. A new scheme which allows one to incorporate specular as well as diffusive interface(s) into the quasiclassical theory is suggested. To make the presentation self-contained, we start with a short introduction to the quasiclassical theory of superconductivity.

As first shown by Bardeen, Cooper, and Schrieffer (BCS) [10], the phenomenon of superconductivity can be understood in the framework of a mean-field type scheme where the Cooper correlations are introduced through the pair potential Δ (generally, a function of the momentum \mathbf{p}) which is related to electron-electron interaction by a self-consistency condition. The mean field Δ may be introduced directly as a kind of Hartree-type potential, or it can be derived in the framework of a more sophisticated Eliashberg theory where the pair potential comes as the anomalous self-energy in the Gor'kov equations for the Green's function. This truly microscopic approach allows one to perform all the normalizations in the spirit of the Landau theory of Fermi liquid and to consider superconductors with a strong coupling (see Seren and Rainer [4] and references therein.)

Whatever the method of derivation, the Gor'kov equation for the matrix Green's function gives the basis for studying the BCS-type superconductivity. The quasiclassical theory of superconductivity offers an approximate simplified scheme of solving the Gor'kov equation. To clarify physics behind the approximations, we analyze first the Bogoliubov - de Gennes equation [10] that is the effective “Schrödinger equation” corresponding to the Gor'kov equation (in the weak coupling limit).

It is well-known that Cooper's pairing in the superconducting state is conveniently described in the language of the electron-hole coherence. On the mean field level, the ground

as well as an excited states of the system are products of single particle states, each of them a quantum superposition of electron and hole. The electron, ψ_e , and hole, ψ_h , amplitudes in the superposition comprise the 2-component single particle wave function, $\Psi(\mathbf{r}, t) = \begin{pmatrix} \psi_e \\ \psi_h \end{pmatrix}$. It obeys the Bogoliubov - de Gennes equation [10],

$$i\hbar \frac{\partial}{\partial t} \begin{pmatrix} \psi_e \\ \psi_h \end{pmatrix} = \begin{pmatrix} \xi(\hat{\mathbf{p}} - \frac{e}{c}\mathbf{A}) + U & \Delta \\ \Delta^* & -\xi(\hat{\mathbf{p}} + \frac{e}{c}\mathbf{A}) - U \end{pmatrix} \begin{pmatrix} \psi_e \\ \psi_h \end{pmatrix} \quad (1.1)$$

where $\xi(\mathbf{p}) = \epsilon(\mathbf{p}) - \mu$, $\epsilon(\mathbf{p})$ and μ being the electron band energy and the chemical potential, respectively, \mathbf{A} is the magnetic vector potential; $U(\mathbf{r})$ is the potential energy. The pairing potential Δ , and, in principle, all other potentials must be found self-consistently.

For future needs we note that in the vicinity of the the Fermi surface $\xi(\mathbf{p}_F) = 0$, the electron (hole) with the momentum $\mathbf{p} \approx \mathbf{p}_F$ moves with the Fermi velocity $\mathbf{v} = +(-)\frac{\partial \xi}{\partial \mathbf{p}_F}|_{\xi=0}$. The particle energy is close to the Fermi energy $E_F \sim vp_F$, and the de-Broglie wave length is λ_F is of order of $\lambda_F \sim \hbar/p_F$, p_F being a typical momentum on the Fermi surface.

In the superconductors which are good metals in the normal state, the potentials are semiclassical (excluding interfaces and disorder which are discussed later) *i.e.* they are slowly varying functions of the coordinate on the scale of the wave length λ_F . Indeed, the pair potential Δ changes at the coherence length $\xi_0 \sim \hbar v/\Delta$, and one estimates the ratio λ_F/ξ_0 as $\lambda_F/\xi_0 \sim \Delta/E_F$. Also, the validity of a semiclassical treatment of magnetic field B requires that $\lambda_F \ll l_B$, l_B being the magnetic length, $l_B = \sqrt{\Phi_0/B}$, $\Phi_0 = hc/2e$. Since superconductivity exists only at $B < B_{c2} \sim \Phi_0/\xi_0^2$, the ratio λ_F/l_B never exceeds Δ/E_F . Seeing that $\Delta \sim T_c$, the semiclassical conditions λ_F/ξ_0 , $\lambda_F/l_B \ll 1$ are equivalent to the requirement that $T_c/E_F \ll 1$. In accordance with the Landau theory of Fermi liquid, this condition is always satisfied if the normal state is metallic.

Most of the physical effects in metals and superconductors (the Hall and thermoelectric effects being notable exceptions) can be described in the simplest approximation where all the corrections of order $T/E_F \sim T_c/E_F$ are neglected *i.e.* in the limit $T_c/E_F \rightarrow 0$. This is the approximation where the quasiclassical theory of superconductivity is valid [4,11].

Since $\frac{T_c}{E_F} \sim \frac{\hbar}{p_F \xi_0}$, the limit is equivalent to $\hbar \rightarrow 0$ or large mass $m \sim p_F/v \rightarrow \infty$. In this limit of quantum mechanics of noninteracting particles, wave packets do not suffer quantum broadening and dynamics becomes completely classical: The particle moves along a trajectory, position $\mathbf{r}(t)$ and momentum $\mathbf{p}(t)$ being well defined. Below we analyse how the electrons-hole coherence in the superconducting state changes the situation.

First, we consider in more detail the classical dynamics of the electron and hole separately. The Bogoliubov - de Gennes equation where we put $\Delta = 0$ for the moment, reads

$$i\hbar \frac{\partial \psi_e}{\partial t} = [\xi(\hat{\mathbf{p}} - e\mathbf{A}) + U] \psi_e, \quad i\hbar \frac{\partial \psi_h}{\partial t} = -[\xi(\hat{\mathbf{p}} + e\mathbf{A}) + U] \psi_h \quad (1.2)$$

The two equations transform into each other after the substitution $t \rightarrow -t$ and $\mathbf{A} \rightarrow -\mathbf{A}$. This means that given a solution $\psi_e(\mathbf{r}, t|\{\mathbf{A}\})$ corresponding to the vector potential \mathbf{A} , the function $\psi_e(\mathbf{r}, -t|\{-\mathbf{A}\})$ solves the equation for ψ_h in the vector potential \mathbf{A} . Therefore,

$$\psi_h(\mathbf{r}, t|\{\mathbf{A}\}) = \psi_e(\mathbf{r}, -t|\{-\mathbf{A}\}), \quad (1.3)$$

provided $\psi_e(\mathbf{r}, t=0) = \psi_h(\mathbf{r}, t=0)$ [12].

If $\hbar \rightarrow 0$, the centre of electron or hole wave packets moves in the $\mathbf{r} - \mathbf{p}$ space along the trajectory specified by the coordinate $\mathbf{r}_{e,h}(t)$ and momentum $\mathbf{p}_{e,h}(t)$ as a function of time t . The relation between electron- and hole-trajectories can be expressed in the following way.

Let $\mathbf{r}_{e(h)}(t|\{\mathbf{b}\})$ together with $\mathbf{p}_{e(h)}(t|\{\mathbf{b}\})$ be the trajectory of the electron (hole) in the magnetic field $\mathbf{b} = \text{rot } \mathbf{A}$. From Eq.(1.3) one can conclude that the corresponding classical dynamics of electrons and holes are related to each other in the following way:

$$\mathbf{r}_h(t|\{\mathbf{b}\}) = \mathbf{r}_e(-t|\{-\mathbf{b}\}) , \quad \mathbf{p}_h(t|\{\mathbf{b}\}) = \mathbf{p}_e(-t|\{-\mathbf{b}\}) \quad (1.4)$$

provided the electron and hole trajectories pass through the same point $\mathbf{r}_e = \mathbf{r}_h = \mathbf{r}_0$ and $\mathbf{p}_e = \mathbf{p}_h = \mathbf{p}_0$ at $t = 0$.

One sees from here that if the magnetic field is absent, $\mathbf{b} = 0$, or its influence on the classical dynamics is negligible, then

$$\mathbf{r}_h(t) = \mathbf{r}_e(-t) , \quad \mathbf{p}_h(t) = \mathbf{p}_e(-t) , \quad (1.5)$$

that is the electron and hole move in opposite directions along the *same* line (path) in the $\mathbf{r} - \mathbf{p}$ space. However, to the extent the magnetic field influences the orbits, the electron and hole paths are *different* [13]. (Obviously, the role of the magnetic field may play any perturbation violating the time reversal symmetry.)

Now we are in position to analyse how the electron-hole mixing (*i.e.* $\Delta \neq 0$ in Eq.(1.1)) changes propagation of the wave packets. Consider a wave packet which is initially purely electronic ($\psi_h = 0$, $t = 0$), and assume for the moment that Eq.(1.5) is valid. The electron moves classically on a trajectory in the $\mathbf{r} - \mathbf{p}$ space, and provides a source, $\Delta^* \psi_e$, in the equation for ψ_h (see Eq.(1.1)) generating a hole wave. Since Δ is a slowly varying field, the source $\Delta^*(\mathbf{r}) \psi_e(\mathbf{r}, t)$ and $\psi_e(\mathbf{r}, t)$ are peaked at the same point of the $\mathbf{r} - \mathbf{p}$ space. In other words, the hole is created at the point of the current position of the electron and with the instantaneous electron momentum. Then, by virtue of Eq.(1.5), the secondary hole moves backwards along the path of the primary electron. In turn, the hole creates new electrons which move along the same path *etc*. It is very important that the multiple processes of the electron-hole conversion keep the packet on a line in the $\mathbf{r} - \mathbf{p}$ space which is nothing but the classical trajectory. However, the width of the packet *along* the trajectory grows linearly in time $\propto vt$ (at times $t > \hbar/\Delta$) due to the reverse of the velocity under the electron \leftrightarrow hole conversion processes.

One sees that, the wave packet in a superconductor experiences broadening even in the limit $\hbar \rightarrow 0$, and, therefore, a quantum description is unavoidable. Nevertheless, the notion of the classical trajectory as a line in the $\mathbf{r} - \mathbf{p}$ space remains meaningful because the quantum broadening occurs only along the line. Ultimately, this important feature is due to the time reversal symmetry. It holds to the extent Eq.(1.5) is accurate *i.e.* when one can neglect the magnetic Lorentz force in the classical dynamics.

Note the peculiar role of a magnetic field: the difference in the magnetic bending of electron and hole trajectories results in the broadening of the coherent electron-hole wave packet in the direction transverse to the classical trajectory. At energies $\sim \Delta$ where the electron and hole components have comparable weight, the significance of the Lorentz force can be estimated [14] from the ratio $\frac{\hbar \omega_c}{\Delta} \lesssim \Delta/E_F$ where $\omega_c = |eB/mc|$ is the cyclotron frequency. Since $\frac{\hbar \omega_c}{\Delta} \propto \frac{1}{m}$, one can consistently neglect the Lorentz since the quasiclassical

theory is effectively a theory of infinitely heavy particles, $m \rightarrow \infty$ as discussed before. It seems that in general case the Lorentz force can be incorporated in a theory of superconductivity only by a full quantum approach (see, however, Kopnin's quasiclassical theory of the Hall effect [15]). Sometimes, the magnetic broadening may turn out to be non-crucial, e.g. in a spatially homogeneous case, and then certain simplifications may be possible (see e.g. [16]).

A more formal and rigorous analysis of electron-hole coherence on classical trajectories can be done using a method first suggested by Andreev [17]. The stationary state wave function is written as $\Psi(\mathbf{r}, t) = \psi(\mathbf{r}) e^{\frac{i}{\hbar} \mathbf{p}_F \cdot \mathbf{r}} e^{\frac{-i}{\hbar} E t}$ where $\psi(\mathbf{r})$ is a slowly varying function (provided $|E| \ll E_F$). Plugging $\Psi(\mathbf{r}, t)$ into the Bogoliubov - de Gennes equation Eq.(1.1), and using the approximation

$$e^{-\frac{i}{\hbar} \mathbf{p}_F \cdot \mathbf{r}} \xi(\hat{\mathbf{p}} - \frac{e}{c} \mathbf{A}) e^{\frac{i}{\hbar} \mathbf{p}_F \cdot \mathbf{r}} \approx \mathbf{v} \cdot \left(\frac{\hbar}{i} \nabla - \frac{e}{c} \mathbf{A} \right)$$

where the small terms of order $(\lambda_F \nabla)^2$ are neglected, one gets the Andreev equation. Rearranging terms, the Andreev equation may be written in the following form

$$\left(i\hbar \mathbf{v} \cdot \nabla + \begin{pmatrix} E - \mathbf{v} \cdot \mathbf{p}_s & \Delta \\ -\Delta^* & -E + \mathbf{v} \cdot \mathbf{p}_s \end{pmatrix} \right) \begin{pmatrix} \psi_e \\ -\psi_h \end{pmatrix} = 0 \quad (1.6)$$

where \mathbf{v} is the velocity at the point \mathbf{p}_F of the Fermi surface, \mathbf{p}_s denotes $\mathbf{p}_s = -\frac{e}{c} \mathbf{A}$ and for simplicity $U = 0$ (as it usually the case because of the efficient screening). The most important feature here is that the derivative $\mathbf{v} \cdot \nabla$ couples the value of the wave function only on straight lines in the direction of the velocity \mathbf{v} ; the lines are the classical trajectories when $U = 0$ [18]. In this approximation, the quantum coherence exists only along the classical trajectories without any coupling between neighbouring paths. These properties are in agreement with the qualitative picture of the wave packet spreading along the classical trajectory, discussed previously. One may call the envelope function ψ in Eq.(1.6) the wave function on the classical trajectory.

After this short review of the quasiclassical approximation, our next step is to include the interface into the scheme. In this introductory part of the paper, we present main ideas using the language of the wave functions on classical trajectory; a more general approach of 2-point trajectory Green's function is presented in Section II.

The reflection/transmission on an isolated interface (a specular one, to begin with) mixes together semi-infinite pieces of classical trajectories (see Fig.1). Each of the pieces is characterized by the Fermi surface momentum \mathbf{p}_F , and the corresponding velocity is \mathbf{v} ; the arrows indicate the direction of the velocity. On pieces of trajectories 1 and 2 the velocity is directed towards the interface, and we call them in-coming trajectories (or channels); correspondingly, 1' and 2' are outgoing (pieces of) trajectories. Throughout the paper, the out-going "channels", alias for "trajectory", are marked by "prime".

Note that the in/out classification of the trajectories in accordance with the direction of the Fermi surface velocity is unique but it is arbitrary because the electron and hole belonging to same channel have the opposite directions of their velocities. For instance, the electron coming to the interface on via e.g. the channel 2 (see Fig. 1) may go away as the electron on trajectories 1' and 2' as well as a hole along nominally in-coming trajectory 1.

We will call “knot” the region inside of which scattering occurs and the pieces of the classical trajectories get “tied” together on the interface [19]. Usually the typical thickness of the interface region is of atomic scale, and only the wave function in the outer region is of interest. Then, on the quasiclassical level of accuracy, the interface (the knot) can be described by the scattering matrix [20]

In general, the knot may tie together arbitrary number, N , of ballistic in-channel to the same number N of the out-channels. For a specular interface, number of channels N equals to 2, and rough interfaces may be modelled by knots with $N > 2$.

The waves generated by a source, e.g. on path 1 in Fig.1, spread to all other paths 1', 2, and 2' coupled by the knot. In the presence of an interface, the wave function on trajectory remains a valid concept if one interprets the notion of trajectory in a broader sense as a set of the points on all the ballistic paths coupled by the knot. For instance, in Fig.1, one understands paths 1, 2, 1', 2' as the parts of a single geometrical object, which we also call a “trajectory”. The spatial argument of the wave function will span the generalized trajectory. Similar constructions are known in the literature: see, e.g. Ref. [21] where the Schrödinger equation is solved on graphs (networks).

The case of many interfaces requires some preliminary remarks. Consider as an example a two layer system Fig.2. *If* the layers are of the same thickness and the reflections are exactly specular, the two outgoing path 1' and 2' meet together again on the upper knot, forming a loop *i.e.* a pair of interfering paths. This causes a major difficulty for the quasiclassical theory: Indeed, the envelope function ψ obeying the Andreev equation is introduced when the phase factor $e^{ip_F \mathcal{L}/\hbar}$, \mathcal{L} being the distance along the path, is singled out of the full wave function. When loops are present and there is more than one path connecting any 2 points, the distance \mathcal{L} is ill-defined, and the procedure of constructing the envelope ψ becomes non-unique and dubious. Besides, the interference phase factors like $e^{ip_F(\mathcal{L}_1 - \mathcal{L}_2)/\hbar}$, $\mathcal{L}_{1,2}$ being the lengths of the interfering paths, crucially sensitive to the value of p_F and cannot be found in the quasiclassical limit where $\hbar/p_F = 0$.

To overcome the difficulty we note the following: The interference leads to Fabri-Perot type geometric resonances and related fluctuations of various physical quantities, perhaps locally strong. However, in the limit $\hbar \rightarrow 0$, the resonances are *close* to each other in the configuration space, and, therefore, the fluctuations are expected to be effectively averaged out when one calculates observables: The latter are given by certain integrals and thus are sensitive mainly to coarse-grain features in the configuration space.

Further, the coarse-grain features (like e.g. the angular-resolved local density of states averaged in small volume ($\gg \lambda_F^3$)) or small interval of directions) are more than likely not perceptive to small variations of geometry shifting the positions of the resonances. Hence, it seems plausible to assume that the coarse-grain structure can be faithfully reproduced if one introduces “virtual roughness”, which is small ($\ll \xi_0$) and not noticeable quasiclassically, and performs averaging with respect to the roughness (kind of ergodic hypothesis). In other words, on the coarse-grain level, an ideal surface is expected to be indistinguishable from a “virtually rough” *i.e.* a random surface with roughness W (see Fig.3) small on the typical quasiclassical scale, $W \ll \xi_0$.

For a rough surface, the picture of trajectories shown in Fig.2 *almost* never occurs: In the quasiclassical approximation, the trajectories are lines with zero ($\sim \lambda_F$) width, and the condition that the trajectories 1' and 2' cross each other again exactly at the interface

(up to $\sim \lambda_F$), is very restrictive. For this, the surfaces must be strictly parallel and the reflections $1' \rightarrow 3$ and $2' \rightarrow 4$ must be specular (identical) with high precision. Qualitatively, the argument here is the same as in the billiard theory where closed orbits are known to be rare exceptions. As long as the loops are absent, solutions to the Andreev equation, vary smoothly when parameters of the trajectory (e.g. its direction) or the surface roughness are changed and have certain limit when the virtual roughness tends to zero. Hence, the averaging with respect to the virtual roughness is trivial: it amounts to neglecting it in any calculation provided the topology of the trajectories is single-connected. The virtual roughness (tending to zero) is needed here only as a mean to eliminate the geometric resonances which are not of interest because they are not seen on the coarse-grain level of description. (Another line of reasoning could be to say that any real sample is always microscopically rough so that loops are statistically impossible).

By these arguments, one comes to the important conclusion that due to the virtual (or real) roughness the paths tied together by a knot do not show any further correlations and do not (*typically*) meet each other on other knots. This seems to be an analog to the impurity averaging. Effectively, it allows one to average over the Fermi wave length scale from the very beginning.

Uncorrelated multiple collisions with interfaces transform a ballistic trajectory into a tree-like geometrical object. To give a general idea of what we mean by a tree, the topological structure of one of the possible trees with $N=2,3$ knots is shown in Fig.4. The tree corresponding to a real physical situation will be presented later.

The main feature of the tree-like trajectory is its one-dimensional character, the property which can equivalently formulated as (i) there is no loops or interfering paths; (ii) there is only one path connecting any two points of the tree; (iii) the cut of any line produces two disconnected pieces.

Since the tree is effectively 1-dimensional, one is able to repeat Andreev's procedure on a tree-like trajectory defining the slowly varying envelope wave $\psi(\mathbf{r})$ by the formula $\Psi(\mathbf{r}) = \psi(\mathbf{r})e^{ip_F \mathcal{L}(\mathbf{r})}$, where \mathbf{r} spans the points on the tree, and $\mathcal{L}(\mathbf{r})$ is the coordinate along the tree counted off a point. In between knots, the Andreev equation Eq.(1.6) is valid and the values of the wave function on a knot are coupled by the scattering S-matrix (see Section III).

The purpose of present paper is to extend the existing quasiclassical Green's function theory of superconductivity to the case of multi-interface geometry. In essence, the standard quasiclassical (" ξ -integrated") theory of superconductivity is the Green's function version of the Andreev equation: Again, the quantum coherence of the electron and hole residing on the same trajectory is taken into full consideration whereas the coherence between particles occupying different trajectories is neglected. The paths are coupled to each other only by the self-consistent effective potentials like various self-energies (impurity, phonon) and the pair potential Δ . The Green function technique has obvious advantages for one is able to perform the disorder averaging, include the inelastic scattering and the strong-coupling effects *etc.*

Although the potential due to crystal imperfections like impurities is far not slowly varying, this does not invalidates the quasiclassical scheme if one is interested only in the disorder averaged properties. It is well-known that the disorder averaging amounts to the impurity self-energy term in the Gor'kov equation which effect is similar to that of the

potential energy. The self-energy varies on the same spatial scale as other self-consistent potential and as such does not violate classicality. Of course, the imaginary part of the self-energy must be small so that the mean free path l is large, $l \gg \lambda_F$. The quantum localization corrections controlled by the parameter $\hbar/p_F l \ll 1$ are ignored, which again is consistent with the limit $\hbar \rightarrow 0$ or $p_F \rightarrow \infty$ accepted in the quasiclassical theory.

We use the version of the quasiclassical theory [22,23] where the main object is the 2-point Green's function on classical trajectories. In our opinion, this approach is most adequate to the above physical picture of the electron-hole phase coherence spreading along classical trajectories. As has already been discussed, in the many-interface geometry the classical trajectory becomes tree-like. Accordingly, the arguments of the 2-point Green's function are points on a tree. In the present paper, we restrict ourselves to the stationary case, and our main concern is the retarded Green's function of the Keldysh technique.

The paper is organized as follows. In Sect.II, we review the quasiclassical theory in the formulation based on the 2-point Green's function. The connection to the standard technique is discussed in Sect.II B. In Sect.II C, we briefly show the connection to the Riccati equation technique [24,25], as well as suggest a general method for the case of a periodic potential. In Sect.III, we derive the boundary conditions for the Green's function on the knot (interface) with arbitrary number of channels. In Sect.IV, a solution to the multi-channel problem of the Andreev reflection as well as the bound states, is given. In Sect.V, we derive the interface boundary condition for the Riccati equation. In Sect.V B, the boundary condition for the Green's function in terms of the transfer matrix is derived. In Sect.VI, we show the usage of the general approach applying the theory for studying simple examples: (i) a film separated by a partially transparent interface from of a bulk material superconductor; (ii) two layers of a finite thickness. Motivated by the recent theory of the paramagnetic effect [26], we pay most attention to the case when the phases of the order parameter in the two superconductors differ in π ; numerical data for the density of states and superfluid density are presented. The results are summarized in Sect.VII. Details of the calculations are collected in the Appendices. In the rest of the paper, $\hbar = 1$.

II. TRAJECTORY 2-POINT GREEN'S FUNCTION

A convenient starting point is the formulation of the quasiclassical technique in terms of the 2-point Green's function on classical trajectories; the method was first suggested in [27] (“ t -representation”), and in a different form developed in [22,23]. The trajectory Green's function is introduced via the following representation of the 2×2 matrix Gor'kov Green's function [28]:

$$G_\varepsilon^R(\mathbf{r}_1, \mathbf{r}_2) = -\frac{m_F}{2\pi} \frac{e^{ip_F|\mathbf{r}_1-\mathbf{r}_2|}}{|\mathbf{r}_1-\mathbf{r}_2|} \hat{g}_+^R(\mathbf{r}_1, \mathbf{r}_2; \varepsilon) + \frac{m_F}{2\pi} \frac{e^{-ip_F|\mathbf{r}_1-\mathbf{r}_2|}}{|\mathbf{r}_1-\mathbf{r}_2|} \hat{g}_-^R(\mathbf{r}_1, \mathbf{r}_2; \varepsilon), \quad p_F|\mathbf{r}_1-\mathbf{r}_2| \gg 1 \quad (2.1)$$

where $m_F = p_F/v$, p_F and v being the Fermi momentum and velocity, respectively; ε in Eq.(2.1) is the energy variable (stationary case). For definiteness, we consider the retarded Green's function G^R of the Keldysh technique. To simplify notations, we assume a spherical Fermi surface; generalization to an anisotropic spectrum is straightforward.

Similar to Andreev's procedure, the fast "quantum" oscillations on the scale λ_F are singled out in Eq.(2.1). Resembling Eq.(1.6), the slowly varying quasiclassical envelopes $\hat{g}_\pm^R(\mathbf{r}_1, \mathbf{r}_2)$ obey first order differential equations [28,22], the gradient term of which couples only the points on straight lines which are obviously the classical trajectories corresponding to a particle on the Fermi surface [29]. The trajectory is specified by its direction \mathbf{n} and arbitrarily chosen initial point \mathbf{R} , so that the position \mathbf{r} of a point on the trajectory \mathbf{R}, \mathbf{n} can be presented as $\mathbf{r} = \mathbf{R} + x\mathbf{n}$, x has the meaning of the coordinate on the trajectory. In the momentum space, the trajectory \mathbf{n} is associated with the points in the vicinity of the Fermi surface where the velocity vector is directed towards \mathbf{n} .

For the trajectory specified by $\{\mathbf{n}, \mathbf{R}\}$, one defines the 2-point Green's function $\hat{g}^R(x_1, x_2 | \mathbf{n}, \mathbf{R})$ [22,23],

$$\hat{g}_\varepsilon^R(x_1, x_2 | \mathbf{n}, \mathbf{R}) = \begin{cases} \hat{g}_+^R(\mathbf{r}_1, \mathbf{r}_2; \varepsilon) & , \quad x_1 > x_2 ; \\ \hat{g}_-^R(\mathbf{r}_1, \mathbf{r}_2; \varepsilon) & , \quad x_1 < x_2 . \end{cases} \quad \mathbf{r}_{1,2} = x_{1,2}\mathbf{n} + \mathbf{R}$$

(In many cases we omit \mathbf{R}, \mathbf{n} and ε for brevity and use the notation $\hat{g}^R(x_1, x_2)$.)

As shown in [22,23], the 2-point Green's function obeys the following equations

$$\left(iv \frac{\partial}{\partial x_1} + \hat{H}_{\varepsilon, \mathbf{n}}^R(\mathbf{r}_1) \right) \hat{g}_\varepsilon^R(x_1, x_2 | \mathbf{n}, \mathbf{R}) = iv\delta(x_1 - x_2) , \quad \mathbf{r}_1 = \mathbf{R} + x_1\mathbf{n} \quad (2.2)$$

$$\hat{g}_\varepsilon^R(x_1, x_2 | \mathbf{n}, \mathbf{R}) \left(-iv \frac{\partial}{\partial x_2} + \hat{H}_{\varepsilon, \mathbf{n}}^R(\mathbf{r}_2) \right) = iv\delta(x_1 - x_2) , \quad \mathbf{r}_2 = \mathbf{R} + x_2\mathbf{n} \quad (2.3)$$

where the 2×2 traceless [30] matrix $\hat{H}_{\varepsilon, \mathbf{n}}^R$,

$$\hat{H}_{\varepsilon, \mathbf{n}}^R = \hat{h}_{\varepsilon, \mathbf{n}}^R - \hat{\Sigma}_{\varepsilon, \mathbf{n}}^R ,$$

$$\hat{h}_{\varepsilon, \mathbf{n}}^R = \begin{pmatrix} \varepsilon - \mathbf{v} \cdot \mathbf{p}_s & \Delta_{\mathbf{n}} \\ -\Delta_{\mathbf{n}}^* & -\varepsilon + \mathbf{v} \cdot \mathbf{p}_s \end{pmatrix} , \quad \mathbf{v} = v\mathbf{n} , \quad (2.4)$$

where $\Delta_{\mathbf{n}}$ is the order parameter (which may dependent on the direction \mathbf{n}), and $\mathbf{p}_s = -\frac{e}{c}\mathbf{A}$, \mathbf{A} being the vector potential, and $\hat{\Sigma}^R$ is built of the impurity self-energy and the part of the electron-phonon self-energy not included to the self-consistent field Δ and .

The boundary condition to Eqs.(2.2), and (2.3) is the requirement that \hat{g}^R is zero at $|x_1 - x_2| \rightarrow \infty$, so that \hat{g}^R is an analytic function of ε in the upper half plane for any $x_{1,2}$ including $|x_1 - x_2| = \infty$.

The advanced Green's function \hat{g}^A is found from Eqs.(2.2) and Eq.(2.3) with \hat{H}^R substituted for \hat{H}^A ,

$$\hat{H}^A = \hat{\tau}_z \left(\hat{H}^R \right)^\dagger \hat{\tau}_z \quad (2.5)$$

where $\hat{\tau}_z$ is the Pauli matrix and the dagger denotes the Hermitian conjugation.

Although the observables can be expressed via the quasiclassical 1-point Green's function ($x_1 = x_2$), the 2-point Green's function turns out to be a useful intermediate object. It gives a full physical description of the system in the approximation where the part of the orbital

degree of freedom is treated classically (no quantum broadening in the plane $\perp \mathbf{n}$), with a complete quantum treatment of the electron-hole degree of freedom.

It is important that the construction based on the notion of smooth classical trajectories remains valid in the presence of disorder (or phonons), in the standard approximation when the scattering is included on the average via the self-energy (provided $p_F l \gg 1$, l being the mean free path).

A. Factorization

To build the Green's function on the trajectory \mathbf{n}, \mathbf{R} , one first considers solutions to the equation

$$\left(iv \frac{\partial}{\partial x} + \hat{H}^R(x) \right) \phi = 0 \quad (2.6)$$

here ϕ is a column, $\phi = \begin{pmatrix} u \\ v \end{pmatrix}$ and \hat{H}^R stands for $\hat{H}_{\varepsilon, \mathbf{n}}^R(\mathbf{r})$ at the trajectory point $\mathbf{r} = x\mathbf{n} + \mathbf{R}$.

Denote $\bar{\psi}$ the row built from a column ψ by the following rule:

$$\bar{\psi} \equiv \psi^T \tau_y \frac{1}{i} \Rightarrow \overline{\begin{pmatrix} u \\ v \end{pmatrix}} = (v, -u) .$$

Note the identities,

$$\bar{\psi}_a \psi_b = -\bar{\psi}_b \psi_a , \quad \bar{\psi}_a \psi_a = 0 , \quad \psi_a \bar{\psi}_b - \psi_b \bar{\psi}_a = (\bar{\psi}_b \psi_a) \hat{1}$$

By virtue of the identity

$$\left(\hat{H}^R \right)^T = -\tau_y \hat{H}^R \tau_y , \quad (2.7)$$

the row $\bar{\phi}(x)$ built from a solution to Eq.(2.6), satisfies the conjugated equation

$$\bar{\phi}(x) \left(-iv \frac{\partial}{\partial x} + \hat{H}^R(x) \right) = 0 \quad (2.8)$$

Combining Eqs.(2.6), and (2.8), one gets the conservation law,

$$\frac{d}{dx} (\bar{\psi}_a \psi_b) = 0 , \quad (2.9)$$

valid for any pair of solutions $\phi_a(x)$ and ϕ_b .

For a general complex ε , the Green's function is built of the regular solutions to Eq.(2.6), *i.e.* solutions satisfying the following boundary conditions

$$\begin{aligned} \phi_+(x) &\rightarrow 0 , \quad x \rightarrow +\infty \\ \phi_-(x) &\rightarrow 0 , \quad x \rightarrow -\infty \end{aligned} \quad (2.10)$$

Denote $\phi_{\pm}^{(N)}$ the normalized solutions for which

$$\bar{\phi}_-^{(N)}(x) \phi_+^{(N)}(x) = 1 . \quad (2.11)$$

The normalization is possible because the l.h.s. is a (finite) constant as it is seen from Eq.(2.9).

The Green's function can be written now as

$$\hat{g}^R(x_1, x_2) = \begin{cases} \phi_+^{(N)}(x_1) \bar{\phi}_-^{(N)}(x_2) & , \quad x_1 > x_2 ; \\ \phi_-^{(N)}(x_1) \bar{\phi}_+^{(N)}(x_2) & , \quad x_1 < x_2 . \end{cases} \quad (2.12)$$

Indeed, it satisfies Eq.(2.2) and Eq.(2.3) at $x_1 \neq x_2$, and is regular at $|x_1 - x_2| \rightarrow \infty$. The normalization in Eq.(2.11) ensures that the discontinuity at $x_1 = x_2$,

$$\hat{g}^R(x+0, x) - \hat{g}^R(x-0, x) = \hat{1} ,$$

is what is required by the δ -function source in Eqs.(2.2), and (2.3).

For clean superconductors with inelastic scattering ignored, $\Sigma^{R(A)} \rightarrow 0$, and Eq.(2.6) is nothing but the Andreev equation Eq.(1.6). Note that the structure of the equations is not changed when the disorder and inelastic scattering is included via the self energies. In this case, however, solutions to Eq.(2.6) have only the meaning of the building block of the Green's functions.

B. 1-point Green's function

Observables can be expressed via the Green's functions with coinciding spatial arguments, and therefore, the 1-point Green's function is the final goal of calculations.

The 1-point Green's functions defined as $\hat{g}_\pm^R(x) = \hat{g}^R(x \pm 0, x)$, can be expressed via the normalized solutions (see Eq.(2.12))

$$\hat{g}_+^R(x) = \phi_+^{(N)}(x) \bar{\phi}_-^{(N)}(x) , \quad \hat{g}_-^R(x) = \phi_-^{(N)}(x) \bar{\phi}_+^{(N)}(x) . \quad (2.13)$$

This expression can be identically written as

$$\hat{g}_+^R(x) = \frac{1}{\bar{\phi}_-(x) \phi_+(x)} \phi_+(x) \bar{\phi}_-(x) , \quad \hat{g}_-^R(x) = \frac{1}{\bar{\phi}_-(x) \phi_+(x)} \phi_-(x) \bar{\phi}_+(x) , \quad (2.14)$$

where the normalization of the wave functions ϕ_\pm is arbitrary.

These matrices are projectors,

$$\hat{g}_\pm^R \hat{g}_\pm^R = \pm \hat{g}_\pm^R , \quad \hat{g}_\pm^R \hat{g}_\mp^R = 0 , \quad \hat{g}_+^R - \hat{g}_-^R = \hat{1} , \quad \text{Sp } \hat{g}_\pm^R = \pm 1 \quad (2.15)$$

Tagging electron- and hole-like excitations in accordance with the direction of their propagation ($\pm x$ directions) and considering examples, e.g. the normal state, one concludes that \hat{g}_+^R can be identified as the (quasi)electron part of the Green's function, and \hat{g}_-^R is the (quasi)hole one (and vice versa for \hat{g}_\pm^A).

Denoting

$$a \equiv \frac{u_-}{v_-} , \quad b \equiv \frac{v_+}{u_+} , \quad (2.16)$$

where u_{\pm} and v_{\pm} are the components of ϕ_{\pm} ,

$$\phi_{\pm}(x) = \begin{pmatrix} u_{\pm}(x) \\ v_{\pm}(x) \end{pmatrix} ,$$

Eq.(2.14) becomes

$$\hat{g}_+^R = \frac{1}{1-ab} \begin{pmatrix} 1 \\ b \end{pmatrix} (1, -a) , \quad \hat{g}_-^R = \frac{1}{1-ab} \begin{pmatrix} a \\ 1 \end{pmatrix} (b, -1) \quad (2.17)$$

Another elucidating form of Eq.(2.14) is as follows

$$\hat{g}_+^R = \hat{O}_{a,b} \begin{pmatrix} 1 & 0 \\ 0 & 0 \end{pmatrix} \hat{O}_{a,b}^{-1} , \quad \hat{g}_-^R = \hat{O}_{a,b} \begin{pmatrix} 0 & 0 \\ 0 & -1 \end{pmatrix} \hat{O}_{a,b}^{-1}$$

where the rotation matrix $\hat{O}_{a,b}$

$$\hat{O}_{a,b} = \begin{pmatrix} 1 & a \\ b & 1 \end{pmatrix} . \quad (2.18)$$

As discussed in [22,23], the 1-point Green's (“ ξ -integrated”) function of the quasiclassical theory, \hat{g}^R , is given by

$$\hat{g}^R = \hat{g}_+^R + \hat{g}_-^R . \quad (2.19)$$

i.e.

$$\hat{g}^R = \phi_+^{(N)} \bar{\phi}_-^{(N)} + \phi_-^{(N)} \bar{\phi}_+^{(N)} . \quad (2.20)$$

In terms of \hat{g}^R ,

$$\hat{g}_{\pm}^R = \frac{1}{2} (\hat{g}^R \pm 1) , \quad (2.21)$$

and the relations in Eq.(2.15) lead to the well-known normalization condition

$$(\hat{g}^R)^2 = \hat{1}$$

and

$$\text{Sp } \hat{g}^R = 0 .$$

Combining Eqs.(2.19) and (2.17), one gets

$$\hat{g}^R = \frac{1}{1-ab} \begin{pmatrix} 1+ab & -2a \\ 2b & -(1+ab) \end{pmatrix} \quad (2.22)$$

This parameterization of the Green's function has been recently suggested by Schopohl and Maki [24] (see, also, [25]). The present derivation leads quite naturally to this decomposition, and clearly shows the physics behind it. Seeing that a and b may be interpreted as the “local” amplitudes of the Andreev reflection for electron and hole (see below), we call them the Andreev amplitudes.

Finally, the rotation with the matrix $\hat{O}_{a,b}$ in Eq.(2.18) diagonalizes \hat{g}^R , i.e.

$$\hat{g}^R = \hat{O}_{a,b} \begin{pmatrix} 1 & 0 \\ 0 & -1 \end{pmatrix} \hat{O}_{a,b}^{-1}$$

The advanced Green's function \hat{g}^A and symmetry relations between \hat{g}^R and \hat{g}^A are discussed in Appendix A.

C. Solving the equation of motion

In this paper we take the approach where the main object of interest is the two component “wave functions” ϕ_{\pm} , which factorizes the Green’s function and obeys the Andreev-type equations. A variety of options can be chosen to find the amplitudes. For future references, some of them are discussed in this section.

1. Riccati equation

Instead of solving linear equations for two component $\phi = \begin{pmatrix} u \\ v \end{pmatrix}$, one solves the equation for the ratio $\alpha = v/u$. It follows from Eq.(2.8) that $\alpha(x)$ satisfies the Riccati equation,

$$i \frac{\partial}{\partial x} \alpha = 2\varepsilon^R \alpha + \Delta^{*R} + \Delta^R \alpha^2 \quad (2.23)$$

where parameters ε^R and Δ^R are found from the identification

$$\hat{H}^R(x) = \begin{pmatrix} \varepsilon^R & \Delta^R \\ -\Delta^{*R} & -\varepsilon^R \end{pmatrix}_x$$

In the context of the quasiclassical theory, this equation has been first derived by Schopohl and Maki [24].

Known $\alpha(x)$, one finds the 2-component function $\phi(x)$,

$$\phi(x) = \text{const} \begin{pmatrix} 1 \\ \alpha(x) \end{pmatrix} \exp \left(i \int_{x_0}^x dx' (\varepsilon^R + \Delta^R \alpha)_{x'} \right) \quad (2.24)$$

To find $\alpha_{\pm}(x)$ *i.e.* the solutions to Eq.(2.23) corresponding to ϕ_{\pm} , the Riccati equation must be supplemented with the boundary condition which leads to the correct asymptotics Eq.(2.10).

In many cases of interest such e.g. an SNS-structure or isolated Abrikosov’s vortex, the superconductor is homogeneous at $x \rightarrow \pm\infty$. If so, solutions to Eq.(2.6) are plane waves in the asymptotic region:

$$\phi(x) \rightarrow \text{conts} \begin{pmatrix} \Delta^R \\ \pm \xi^R - \varepsilon^R \end{pmatrix} e^{\pm i \xi^R x}$$

$\xi^R = \sqrt{(\varepsilon^R)^2 - \Delta^R \Delta^{*R}}$, $\Im \xi^R > 0$. Selecting the waves decaying in the corresponding region, one comes to the boundary conditions as follows:

$$\phi_{\pm} : \quad \alpha_{\pm}|_{x=\pm\infty} = \frac{\pm \xi^R - \varepsilon^R}{\Delta^R}|_{x=\pm\infty} \quad (2.25)$$

An equivalent condition was suggested in [24,25] from “the requirement of the stability of the numerical integration procedure”. In the present paper, the boundary condition is deduced,

ultimately, from the physical condition that the 2-point Green's function is a regular function decaying at large distance from the source.

The 1-point Green's functions \hat{g}_\pm^R and \hat{g}^R are found now from Eq.(2.17) and Eq.(2.22) with the understanding that

$$b(x) = \alpha_+(x) , \quad a(x) = 1/\alpha_-(x)$$

where $\alpha_\pm(x)$ are the solutions to Eq.(2.23) with the boundary conditions in Eq.(2.25).

2. Periodic potential

In many situations of interest such us vortex lattice, N-S or S-S superlattice, or multiple reflections (see below) the potentials are periodic functions of the trajectory coordinate. In this case, the Green's functions may be found by the following method.

A formal solution to Eq.(2.6), $\phi(x) = \hat{U}(x, x_0)\phi(x_0)$, can be expressed via the evolution matrix

$$\hat{U}(x, x_0) = T_x e^{-i \int_{x_0}^{x_1} dx' \hat{H}^R(x')}$$

where T_x orders the matrices $\hat{H}^R(x)$ in the descending x -order from the left to the right.

Denote $\hat{U}_L(x) \equiv \hat{U}(x + L, x)$ the evolution matrix corresponding to the translation by the period of the structure L . As proven in Section B, the 1-point Green's function can be found as

$$\hat{g}^R(x) = \mathcal{F}_R \left[\hat{U}_L(x) \right] . \quad (2.26)$$

Here $\mathcal{F}_R [\dots]$ stands for the “formating” operation:

$$\mathcal{F}_R \left[\hat{Q} \right] = \frac{1}{q_R} \left(\hat{Q} - \left(\frac{1}{2} \text{Sp} \hat{Q} \right) \hat{1} \right) , \quad q_R = \sqrt{\left(\hat{Q} - \left(\frac{1}{2} \text{Sp} \hat{Q} \right) \hat{1} \right)^2} , \quad (2.27)$$

which returns a normalized traceless matrix [31] (similar combination of matrices has been introduced in [8]). The branch of the square root in q_R must be chosen to satisfy $\Re(\mathcal{F}_R[\hat{Q}])_{11} > 0$. Except for the choice of the branch, Eqs.(2.26), and (2.27) are same for \hat{g}^A . Construction of the evolution matrix $\hat{U}_L(x)$ in the Riccati equation technique is described in Section B.

III. KNOT MATCHING CONDITIONS

In the quasiclassical picture, particles move on trajectories, usually, straight lines characterized by the direction of velocity \mathbf{n} (and the initial position \mathbf{R}). At any point in real space, infinite number of trajectories with different \mathbf{n} cross each other. Since there is no transitions between the intersecting trajectories, the crossings do not lead to any physical effect. At some points, called here knots, the quasiclassical condition is violated. At a knot,

the particle may leave its original trajectory and continue its motion along a trajectory in another direction. In the simplest example of a specular interface Fig. 1, two trajectories 1-1' and 2-2' are mixed. In a general case, the knot is a region where transitions between N in- and N out-trajectories are allowed. The in- trajectories (or channels) are those which have the direction of the Fermi momentum towards the knot; the momentum direction is from the knot in the out-channels (see Fig. 4) [32]. The in- and out-trajectories are somehow numbered, $l = 1, \dots, N$. We mark by ' the out-going channels so that k' stands for the k -th outgoing channels.

Since the knot is point-like on the quasiclassical scale $\sim v_F/\Delta$, one can talk about the knot value of the trajectory “wave function”. Denote ψ_i the 2-component wave function on the i -th in-coming trajectory, $i = 1, \dots, N$ at the point where it enters the knot, and analogously $\psi_{k'}$ the knot value on the k -th outgoing trajectory.

The outcome of events happening inside the knot can be generally described by the scattering S-matrix. For any specified case, it can be found by solving the Schrödinger equation for the electron with the Fermi energy. Here, it is considered as a phenomenological input.

The suggested matching condition reads

$$\psi_{k'} = \sum_{i=1}^N S_{k'i} \psi_i, \quad (3.1)$$

where $S_{k'i}$ are the elements of the unitary scattering matrix. In the spirit of the quasiclassical theory, $S_{k'i}$ is the normal metal property taken at the Fermi surface; it is an electron-hole scalar. This relation generalizes the matching conditions of Ref. [20] to the many channels case.

Taking advantage of unitarity, $S^{-1} = S^\dagger$, the inverse of Eq.(3.1) reads

$$\psi_i = \sum_{k'=1}^N S_{ik'}^\dagger \psi_{k'} \quad (3.2)$$

Seeing that the conjugated wave function $\bar{\psi}$ always belongs to the second argument of the Green's function $G(1, 2) \sim \langle \psi(1) \psi^*(2) \rangle$, it must obey the matching conditions for ψ^* *i.e.*

$$\bar{\psi}_{k'} = \sum_{i=1}^N S_{k'i}^* \bar{\psi}_i \quad (3.3)$$

Eq.(2.6) together with the matching conditions in Eq.(3.1), allows one to find the 2-component amplitudes on the tree-like trajectory, and, therefore, the Green's functions. We remark also that the relation in Eq.(3.1) can be used as the boundary condition to the Andreev equation 1.6.

IV. ANDREEV REFLECTION ON THE KNOT

In this section, we consider the quantum problem of scattering of ballistic excitations off the knot or, in other words, the problem of many-channel combined, Andreev and usual,

reflection/transmission. The problem is formulated as follows. On each of the trajectories connected by the knot, $i, k' = 1, 2, \dots, N$, the order parameter $\Delta(x)$ and, hence, the matrix $\hat{h}(x)$ in Eq.(2.4) is supposed to be known. Since in the ballistic case $\Sigma = 0$, the wave function on each of the trajectories satisfies the equation

$$\left(iv \frac{\partial}{\partial x} + \hat{h}(x) \right) \psi = 0 , \quad (4.1)$$

here x is the coordinate along the corresponding trajectory; this equation differs only in notations from the Andreev equation Eq.(1.6). The scattering of the (quasi)particles off the knot is due multiple sequential processes of (i) inter-trajectory transitions described by Eq.(3.1), which do not affect the the electron-hole degrees of freedom, followed by (ii) intra-trajectory Andreev reflections i.e. rotations in the electron-hole space. The goal is to express the amplitudes of the multiple processes via the amplitudes of the elementary events.

On each of the paths, we chose the origin $x = 0$ at the knot. Then, the coordinate x belongs to the region $-\infty < x < 0$ on the in-coming and to the region $0 < x < \infty$ on the outgoing trajectories.

First, we consider the plane wave asymptotics at $|x| \rightarrow \infty$ where $\hat{h} = \text{const}(x)$. The electron-like (hole-like) solution is $\Psi_e(x) = \psi_e e^{i\xi x/v}$ ($\Psi_h(x) = \psi_h e^{-i\xi x/v}$), where ψ_e (ψ_h), $\hat{h}\psi_e = +\xi\psi_e$ ($\hat{h}\psi_h = -\xi\psi_h$) is the eigenfunction of the matrix \hat{h} . The eigenvalues $\pm\xi$ are found from $\xi^2 \hat{1} = \hat{h}^2$. We supply the energy with an infinitesimal *positive* imaginary part, $\varepsilon \rightarrow \varepsilon + i\delta$, and impose condition $\Im\xi > 0$ to specify the branch of $\sqrt{\xi^2}$.

The basis for the electron-hole classification is the quasiparticle current

$$j_{qp} = \psi^\dagger \hat{\tau}_z \psi = |u|^2 - |v|^2 \quad (4.2)$$

which is a constant of motion, $\frac{d}{dx} j_{qp}(x) = 0$, due to the symmetry $\hat{h}^\dagger = \hat{\tau}_z \hat{h} \hat{\tau}_z$. The electron-like quasiparticle is identified by $j_{qp} > 0$. It moves in the direction of increasing x in accordance with the sign of the probability current. For the hole-like excitation $j_{qp} < 0$, and it moves towards $x = -\infty$. Note that the solution $\Psi^{(e,h)}$ are chosen in the way that both electron and holes decay in the direction of propagation.

Below, $\psi^{(e,h)}$ denotes the eigenfunctions normalized to the unit flux:

$$\psi^{(e)\dagger} \hat{\tau}_z \psi^{(e)} = 1 , \quad \psi^{(h)\dagger} \hat{\tau}_z \psi^{(h)} = -1 , \quad \xi^2 > 0 .$$

(The l.h.s. is identically zero in the gap region when $\xi^2 < 0$ and propagating states are absent.)

Generally, \hat{h} is x -dependent and the solutions are the plane waves only asymptotically. However, the electron-hole classification is unique due to the current conservation in Eq.(4.2). One has for the electron- , $\Psi^{(e)}(x)$, and hole-like, $\Psi^{(h)}(x)$, solutions on out-going (in-coming) trajectories

$$\Psi^{(e)}(x) = \begin{cases} \psi^{(e)} e^{i\xi x/v} , & x \rightarrow \infty \text{ (or } -\infty\text{)} ; \\ \frac{1}{\beta^{(e)}} \begin{pmatrix} 1 \\ \alpha^{(e)} \end{pmatrix} , & x = 0 . \end{cases} \quad (4.3)$$

$$\Psi^{(h)}(x) = \begin{cases} \psi^{(h)} e^{-i\xi x/v} & , \quad x \rightarrow \infty \text{ (or } -\infty\text{)} ; \\ \frac{1}{\beta^{(h)}} \begin{pmatrix} \alpha^{(h)} \\ 1 \end{pmatrix} & , \quad x = 0 . \end{cases} \quad (4.4)$$

where the parameters $\alpha^{(e,h)}$ and $\beta^{(e,h)}$ are found solving Eq.(4.1) in the region $0 < x < \infty$ (or $-\infty < x < 0$).

If considered as a function of x , $\alpha^{(e)}(x)$ and $1/\alpha^{(h)}$ can be found by solving Eq.(2.23). We see that indeed the parameters $a(x)$ and $b(x)$ of the Riccati equation technique have the meaning of the instantaneous (local) amplitudes of Andreev reflection, and, therefore, one may call them the Andreev amplitudes.

It generally follows from the current conservation Eq.(4.2) that

$$\alpha^{(h)} = (\alpha^{(e)})^* , \quad |\alpha^{(e)}|^2 + |\beta^{(e)}|^2 = |\alpha^{(h)}|^2 + |\beta^{(h)}|^2 = 1 .$$

for an open channel, $\xi^2 > 0$. Seeing that $|\beta^{(e)}|^2 = |\beta^{(h)}|^2$, one can enforce

$$\beta^{(e)} = \beta^{(h)}$$

choosing the overall phase factor in $\psi^{(e,h)}$.

The physical meaning of the parameters is clear from Eqs.(4.3), and (4.4): On the outgoing trajectories ($0 < x < \infty$), $\alpha^{(e)}$ is the amplitude of the Andreev reflection of the (bare) electron injected at $x = 0$, and $\beta^{(e)}$ is the corresponding transmission amplitude; $\alpha^{(h)}/\beta^{(h)}$ and $1/\beta^{(h)}$ are $u-, v-$ components of the quasi-hole having come from $x = \infty$. On the in-coming paths, the above is true after the substitution “electron” \leftrightarrow “hole”.

Moving towards the knot, quasi-electrons on the in-coming and quasi-holes on the outgoing trajectories comprise the in-coming states of the scattering problem; the out-going states are electrons on the out-going and holes excitations on the in-coming trajectories.

Let the incoming particle be the quasi-electron approaching the knot along the l -th in-trajectory. The source particle generates waves in *all* out-going channels. The wave functions of the system $\Psi^{(l)}$ reads

$$\Psi^{(l)} = \Psi_l^{(e)} + B_l^{(l)} \Psi_l^{(h)} + \sum_{k \neq l} B_k^{(l)} \Psi_k^{(h)} + \sum_{k'} A_{k'}^{(l)} \Psi_{k'}^{(e)} \quad (4.5)$$

where $\Psi_{k'}^{(e)}$ and $\Psi_k^{(h)}$ stands for the trajectory wave functions defined by Eqs.(4.3), and (4.4), k or k' being the label of the trajectory. The yet unknown amplitudes of the outgoing particles, $A_{k'}^{(l)}$ and $B_k^{(l)}$, are to be found from the matching conditions in Eq.(3.1).

The calculations are most easily done using Eqs.(C6), and (C7). It follows by comparing Eq.(C6) with Eqs.(4.3), (4.4), that one may put $\nu_{m \neq l} = \alpha_m^{(h)}$ and $\mu_{k'} = \alpha_{k'}^{(e)}$. From Eq.(C6) and Eq.(C4), one sees that the wave functions on the source trajectory at $x_l = 0$ must be proportional to $(\alpha_{0l}^{(e)})$, where

$$\alpha_{0l}^{(e)} = \langle l | S^\dagger \hat{\alpha}^{(e)} \hat{\mathbf{S}}_l | l \rangle . \quad (4.6)$$

Here and below, $\hat{\mathbf{S}}_l$, is the full S-matrix taking into account multiple events of the Andreev reflection. From Eq.(C5)

$$\hat{\mathbf{S}}_l = \left(\hat{S}^\dagger - (\hat{\alpha}^{(h)})^{(l)} \hat{S}^\dagger \hat{\alpha}^{(e)} \right)^{-1} ; \quad (4.7)$$

where $\hat{\alpha}^{(e,h)}$ is the diagonal matrix with the elements $(\hat{\alpha}^{(e,h)})_{kk} = \alpha_k^{(e,h)}$ and superscripts (l) means the ll -element must be put to zero. By $\langle l|Z|m \rangle$, $l, m = 1, \dots, N$ we denote the matrix element Z_{lm} .

The parameter $\alpha_{0l}^{(e)}$ in Eq.(4.6) has the meaning of the amplitude of the Andreev backscattering of a bare electron by the knot as a whole. From the condition that the wave function has the $u - v$ structure at $x_l = 0$ like $\begin{pmatrix} 1 \\ \alpha_{0l}^{(e)} \end{pmatrix}$, one finds B_l , *i.e.* the amplitude of the Andreev reflection of the incident electron excitation. After some algebra

$$B_l^{(l)} = \frac{\alpha_{0l}^{(e)} - \alpha_l^{(e)}}{1 - \alpha_{0l}^{(e)} \alpha_l^{(h)}} . \quad (4.8)$$

Here, the denominator can be understood as due to multiple Andreev reflections [33].

The wave function $\Psi_l^{(e)} + B_l^{(l)} \Psi_l^{(h)}$ at $x_l = 0$ equals now to $C \begin{pmatrix} 1 \\ \alpha_{0l}^{(e)} \end{pmatrix}$ where $C = \beta_l^{(e)*} \left(1 - \alpha_{0l}^{(e)} \alpha_l^{(h)} \right)^{-1}$. Looking at Eq.(C6), one finds the rest of the scattering amplitudes:

$$A_{k'}^{(l)} = \frac{1}{1 - \alpha_{0l}^{(e)} \alpha_l^{(h)}} \langle k' | \hat{\beta}^{(e)} \hat{\mathbf{S}}_l \hat{\beta}^{(e)*} | l \rangle , \quad B_k^{(l)} = \frac{1}{1 - \alpha_{0l}^{(e)} \alpha_l^{(h)}} \langle k | \hat{\beta}^{(h)} \hat{S}^\dagger \hat{\alpha}^{(e)} \hat{\mathbf{S}}_l \hat{\beta}^{(e)*} | l \rangle . \quad (4.9)$$

Similarly, one derives the scattering amplitudes for the quasi-hole coming to the knot on the n' -trajectory. Analogously to Eq.(4.5), the wave function,

$$\Psi^{(n')} = \Psi_{n'}^{(h)} + B_{n'}^{(n')} \Psi_{n'}^{(e)} + \sum_{k' \neq n'} B_{k'}^{(n')} \Psi_{k'}^{(e)} + \sum_k A_k^{(n')} \Psi_k^{(h)} ,$$

contains the scattering amplitudes which are found from the matching conditions. The corresponding expressions can be obtained by the substitutions: $(e) \leftrightarrow (h)$, $l \rightarrow n'$, and $S \leftrightarrow S^\dagger$, and $\mathbf{S}_l \rightarrow \mathbf{S}_{n'}^\dagger$,

$$\hat{\mathbf{S}}_{n'}^\dagger = \left(\hat{S} - (\hat{\alpha}^{(e)})^{(n')} \hat{S} \hat{\alpha}^{(h)} \right)^{-1} .$$

For the hole incident on the n' -trajectory, the amplitudes of the Andreev reflection, $B_{n'}^{(n')}$, scattering to the hole state on the k -th trajectory, $A_k^{(n')}$, and scattering to the electron state on the k' -th trajectory, $B_{k'}^{(n')}$, read respectively

$$B_{n'}^{(n')} = \frac{\alpha_{0n'}^{(h)} - \alpha_{n'}^{(h)}}{1 - \alpha_{0n'}^{(h)} \alpha_{n'}^{(e)}} , \quad (4.10a)$$

$$A_k^{(n')} = \frac{1}{1 - \alpha_{0l}^{(h)} \alpha_l^{(e)}} \langle k | \hat{\beta}^{(h)} \hat{\mathbf{S}}_{n'}^\dagger \hat{\beta}^{(h)*} | n' \rangle \quad (4.10b)$$

$$B_{k'}^{(n')} = \frac{1}{1 - \alpha_{0l}^{(h)} \alpha_l^{(e)}} \langle k' | \hat{\beta}^{(e)} S \hat{\alpha}^{(h)} \hat{\mathbf{S}}_{n'}^\dagger \hat{\beta}^{(h)*} | n' \rangle \quad (4.10c)$$

The presented formulae give the amplitude of scattering from a propagating channel to another propagating channel. The scattering of the excitations is a result of multiple sequential events of two types: (i) on the knot inter-trajectory transitions described by the S -matrix in Eq.(3.1), and (ii) intra-trajectory processes of the Andreev reflection/transmission with the amplitudes $\alpha^{(e,h)}/\beta^{(e,h)}$. Expanding the effective S -matrix \mathbf{S}_l in Eq.(4.7), $\mathbf{S}_l = \hat{S} + \hat{S}(\hat{\alpha}^{(h)})^{(l)} \hat{S}^\dagger \hat{\alpha}^{(e)} \hat{S} + \hat{S}(\hat{\alpha}^{(h)})^{(l)} \hat{S}^\dagger \hat{\alpha}^{(e)} \hat{S}(\hat{\alpha}^{(h)})^{(l)} \hat{S}^\dagger \hat{\alpha}^{(e)} \hat{S} + \dots$ one sees that the full amplitude of the scattering event $n' \leftarrow m$ is the superposition of all different paths connecting the initial and final states with electron \leftrightarrow hole transformation on each step.

The theory gives exact amplitudes of the multiple scattering expressed via the amplitudes of the elementary processes: the normal metal S -matrix and the intra-trajectory Andreev amplitudes. In the simplest case, when $N = 2$, and $\Delta = 0$ on two out of the 4 trajectories, the above formula reproduce results of the theory of Andreev reflection in the NIS structure [22].

A. Bound states

Bound states are physical solutions existing in the absence of a source. The physical solutions are those when the matching conditions on the knot are simultaneously satisfied with the requirement that the wave functions decay far away from the knot. The electron and holes states defined earlier (with $\Im\xi > 0$) have the property that they decay in the direction of their propagation. Therefore, the wave function of a bound state Ψ_{bound} has the form

$$\Psi_{\text{bound}} = \sum_k B_k \Psi_k^{(h)} + \sum_{k'} A_{k'} \Psi_{k'}^{(e)}$$

where the coefficients A 's and B 's are found from the matching conditions. Again, looking at Eqs.(4.3), and (4.4) one sees that in Eq.(C1), $\mu_{k'}$ may be identified with $\alpha_{k'}^{(e)}$, and ν_i with $\alpha_i^{(h)}$. Then, Eq.(C3),

$$\mathcal{D}(\{\alpha^{(h)}\}, \{\alpha^{(e)}\}) \equiv \det \left| \left| 1 - \hat{S} \hat{\alpha}^{(h)} \hat{S}^\dagger \hat{\alpha}^{(e)} \right| \right| = 0, \quad (4.11)$$

gives the condition for the wave functions to be matched on the knot. The Andreev amplitudes $\alpha^{(e)}$ and $\alpha^{(h)}$ are functions of energy ε , and the bound states exist at the energies where Eq.(4.11) is satisfied.

B. Example: Rough surface, anisotropic superconductor

The rough surface reflects waves in many direction. As the simplest model, we assume that the surface reflection couples together only 2 in-coming directions "1" and "2" to two outgoing "1" and "2". The model corresponds to a $N = 2$ knot. In what follows we calculate the amplitude of Andreev reflection by the knot and consider the bound levels.

The unitary 2×2 scattering matrix of the knot may be taken in the form

$$\hat{S} = \begin{pmatrix} r_1 & r_2 \\ -r_2^* & r_1^* \end{pmatrix}$$

provided $R_1 + R_2 = 1$, where $R_1 = |r_1|^2$ ($R_2 = |r_2|^2$) is the probability of reflection $1 \rightarrow 1'$ ($2 \rightarrow 2'$).

Given the profile of the order parameter, one can find the wave functions, and the Andreev amplitudes $\alpha^{(e,h)}$ and $\beta^{(e,h)}$. Here, the matrices

$$\hat{\alpha}^{(h)} = \begin{pmatrix} \alpha_1^{(h)} & 0 \\ 0 & \alpha_2^{(h)} \end{pmatrix}, \quad \hat{\alpha}^{(e)} = \begin{pmatrix} \alpha_{1'}^{(e)} & 0 \\ 0 & \alpha_{2'}^{(e)} \end{pmatrix},$$

are taken as input, each of the α 's is a functions of energy.

The energies of bound states are found from Eq.(4.11), which takes the following form

$$\mathcal{D}(\varepsilon) \equiv R_1(1 - \alpha_1^{(h)}\alpha_{1'}^{(e)})(1 - \alpha_2^{(h)}\alpha_{2'}^{(e)}) + R_2(1 - \alpha_1^{(h)}\alpha_{2'}^{(e)})(1 - \alpha_2^{(h)}\alpha_{1'}^{(e)}) = 0. \quad (4.12)$$

The bound states exist only in the gap region at the energy interval where $|\alpha_{1,2}^{(h)}| = |\alpha_{1',2'}^{(e)}| = 1$.

Essential physics can be grasped by the simplest model where the order parameter Δ_n is a constant at each of the trajectories: $\Delta_n = \Delta e^{i\varphi_n}$. Then,

$$\alpha_{1',2'}^{(e)} = e^{\frac{i}{2}\psi} e^{-i\varphi_{1',2'}}, \quad \alpha_{1,2}^{(h)} = e^{\frac{i}{2}\psi} e^{i\varphi_{1,2}}$$

where ψ_ε is a function of energy, $e^{i\psi_\varepsilon} = (\varepsilon - i\sqrt{|\Delta|^2 - \varepsilon^2})/(\varepsilon + i\sqrt{|\Delta|^2 - \varepsilon^2})$.

Eq.(4.12) is conveniently transformed to the form,

$$\cos(\psi_\varepsilon + \varphi_{11'} + \varphi_{22'}) = R_1 \cos\left(\frac{\varphi_{12} - \varphi_{1'2'}}{2}\right) + R_2 \cos\left(\frac{\varphi_{12} + \varphi_{1'2'}}{2}\right), \quad (4.13)$$

$$\varphi_{ab} \equiv \varphi_a - \varphi_b.$$

One sees that the existence and position of the bound state is sensitive to the surface roughness only if either the incoming or outgoing channels are not equivalent *i.e.* $\varphi_{12} = \varphi_1 - \varphi_2 \neq 0$, or $\varphi_{1'2'} = \varphi_{1'} - \varphi_{2'} \neq 0$. In other words, mixing of identical channel does not affects the levels.

Consider now the possibility, which may exist in the case of a d-wave superconductor, that the order parameter changes its sign on the $1 \rightarrow 1'$ and $2 \rightarrow 2'$ trajectories. A smooth surface mixes only trajectories with close transverse momenta; then the trajectories are almost equivalent and their coupling does not shift the levels. On the contrary, a backward-like scattering splits the degenerate levels: In the model under consideration, the backward-like scattering corresponds to the phase factors $\varphi_1 = \varphi_{2'} = \pi$ and $\varphi_2 = \varphi_{1'} = 0$. Then, from Eq.(4.13) $\cos \psi_\varepsilon = R_2 - R_1$. The bound state energies are

$$\varepsilon_{\text{bound}} = \pm \sqrt{R_2} \Delta. \quad (4.14)$$

One concludes that the presence of substantial spectral weight at low energies is not likely if scattering in the backward directions is present: $\sim 10\%$ probability the scattering moves the levels from zero energy to $\sim 0.3\Delta$, of the order of the gap.

The amplitudes of scattering of excitations can be found from Eqs.(4.8), (4.9) and (4.10c). As an example, the amplitude of the Andreev reflection of the electron-like excitation incident on the trajectory “1”, $B_1^{(1)}$, reads

$$B_1^{(1)} = \frac{R_1 \tilde{\alpha}_{1'}^{(e)} - \tilde{\alpha}_1^{(e)}}{1 - R_1 \tilde{\alpha}_{1'}^{(e)} \tilde{\alpha}_1^{(h)}} .$$

where the following notations are used

$$\begin{aligned}\tilde{\alpha}_1^{(h)} &= \frac{\alpha_1^{(h)} - \alpha_2^{(h)}}{1 - \alpha_{2'}^{(e)} \alpha_1^{(h)}} , \\ \tilde{\alpha}_{1'}^{(e)} &= \frac{\alpha_{1'}^{(e)} - \alpha_{2'}^{(e)}}{1 - \alpha_{1'}^{(e)} \alpha_2^{(h)}} , \\ \tilde{\alpha}_1^{(e)} &= \frac{\alpha_1^{(e)} - \alpha_{2'}^{(e)}}{1 - \alpha_1^{(e)} \alpha_2^{(h)}} .\end{aligned}$$

The shortest way to derive this result is to apply the rotation transforming $\alpha_2^{(h)}$ and $\alpha_{2'}^{(e)}$ to zero as explained in Section D.

V. MATCHING GREEN'S FUNCTIONS

As has been discussed in Section II A and II B, the Green's functions can be built from the regular solutions to the Andreev equation Eq.(2.6). When the trajectory coordinate x extends from $-\infty$ to ∞ , the regularity requirement leads to the boundary conditions in Eq.(2.10). In the case of a trajectory ending in or originating from a knot the boundary conditions must be reformulated.

First consider an isolated knot mixing semi-infinite trajectories (with no more knots on them). With the origin chosen at the knot, the trajectory coordinate x_n extends from $-\infty$ to 0 on the n -th incoming trajectory, and $0 < x_{k'} < \infty$ on the k' -outgoing one. As before, the requirement,

$$\phi_{-,m}(-\infty) = 0 , \quad \phi_{+,k'}(\infty) = 0 , \quad m, k = 1, \dots, N , \quad (5.1)$$

uniquely (up to a normalization factor) defines the solutions $\phi_{-,n}(x_n)$ and $\phi_{+,k'}(x_{k'})$. Denote the knot values of the regular solutions as

$$\phi_{-,m}(x_m = 0) = \begin{pmatrix} a_m \\ 1 \end{pmatrix} , \quad \phi_{+,k'}(x_{k'} = 0) = \begin{pmatrix} 1 \\ b_{k'} \end{pmatrix} , \quad m, k = 1, \dots, N . \quad (5.2)$$

For convenience, the normalization is chosen so that one of the components equals to 1 at the knot; the parameters a_m or $b_{k'}$ are “bulk” properties independent on the knot.

The problem in hand is to find the knot values

$$\phi_{+,l}(x_l = 0) \equiv \begin{pmatrix} 1 \\ b_l \end{pmatrix} , \quad \phi_{-,n'}(x_{n'} = 0) \equiv \begin{pmatrix} a_{n'} \\ 1 \end{pmatrix} , \quad l, n = 1, \dots, N$$

which give the boundary condition to Eq.(2.6) needed to evaluate $\phi_{+,l}(x_l < 0)$ and $\phi_{-,n'}(x_{n'} > 0)$.

To find $\phi_{+,l}(0)$, one notes that by virtue of the matching conditions in Eq.(3.1) and Eq.(3.2), a finite $\phi_{+,l}(0)$ generates waves in all other channels, outgoing and incoming. In

a regular solution, all the secondary waves must decay while propagating from the knot. This condition fixes the $u - v$ structure of the secondary waves: in each of the channel, the incoming $m \neq l$ and any outgoing one k' , the generated 2-component wave functions (at $x = 0$) must be proportional to that in Eq.(5.2). As proven in Section C, the matching condition allows one to find the $u - v$ structure in one of the channels provided, as is the case here, it is known for all other channels.

Changing notions in formulae in Section C ($\mu_{k'} \rightarrow b_{k'} , \nu_{i \neq l} \rightarrow a_i , \nu_{l-1} = b_l$), one gets from Eq.(C4)

$$b_l = \langle l | \hat{S}^\dagger \hat{b} \hat{\mathbf{S}}_l | l \rangle \quad (5.3)$$

where

$$\hat{\mathbf{S}}_l = \left(\hat{S}^\dagger - \hat{a}^{(l)} \hat{S}^\dagger \hat{b} \right)^{-1} ,$$

$\hat{a} = \text{diag}(a_1, a_2, \dots)$ and $\hat{b} = \text{diag}(b_{1'}, b_{2'}, \dots)$; the superscript (l) has the meaning that the l -th element on the diagonal must be put to zero; and $\langle l | (\dots) | l \rangle \equiv (\dots)_l$.

Repeating the arguments, one finds the boundary value $a_{n'}$. Changing notations in Eq.(C8) ($\mu_{n'}^{-1} \rightarrow a_{n'}$), one gets

$$a_{n'} = \langle n' | \hat{S} \hat{a} \hat{\mathbf{S}}_{n'}^\dagger | n' \rangle . \quad (5.4)$$

where

$$\hat{\mathbf{S}}_{n'}^\dagger = \left(\hat{S} - \hat{b}^{(n')} \hat{S} \hat{a} \right)^{-1} ,$$

From the derivation in Section C, it is clear that both Eq.(5.3) and 5.4 are just different forms of Eq.(C3), which reads in the present notations

$$\mathcal{D}(\{a\}, \{b\}) \equiv \det \left| \left| 1 - \hat{S} \hat{a} \hat{S}^\dagger \hat{b} \right| \right| = 0 . \quad (5.5)$$

This equation should be understood in the following sense:

Suppose one seeks for the boundary value of b_l for the l -the in-channel. Then, one formally solves Eq.(5.5) relative to a_l , the obtained value (the inverse of the r.h.s. Eq.(5.3)) gives b_l^{-1} . In the same manner, one finds the knot value of $a_{k'}$ on the k' -outgoing trajectory as the inverse of the root of Eq.(5.5) relative to $b_{k'}$. The procedure does not pose calculational problems since the determinant is a linear function of any of a 's or b 's. Eq.(5.5) represents most concise and symmetric form of the boundary condition to Eq.(2.6).

Summarizing, the Green's functions on trajectories linked by a knot is calculated in the following scheme. First, one solves Eq.(2.6) with boundary condition in Eq.(5.1) on each of the trajectories and calculates functions $\phi_{-,m}(x < 0)$ and $\phi_{+,k'}(x > 0)$; the parameters a_m and $b_{k'}$ in Eq.(5.2) are then also known. The next step is to calculate the knot value of b 's on the incoming trajectories and a 's on the outgoing ones. This is done by formulae in Eq.(5.3) and Eq.(5.4). Having obtained the boundary values, one solves Eq.(2.6) for $\phi_{+,m}(x < 0)$ on the incoming trajectories and $\phi_{-,k'}(x > 0)$ on the outgoing ones. The 1-point Green's function is then built from ϕ_{\pm} by the recipe in Eq.(2.20).

In the Riccati equation technique, one first finds the Andreev amplitudes $a_m(x)$ and $b_{k'}(x)$, $m, k = 1, \dots, N$ from Eqs.(2.23,2.25). Then, Eqs.(5.3), and (5.4) provide the initial value for $b_m(x)$ and $a_{k'}(x)$, solutions to the Riccati equation. The Green's function is then given by Eq.(2.22).

The matching conditions can be also expressed via the transfer matrix as derived in Section VB and in the case of a $N = 2$ knot explained in detail in Section E.

This scheme is also applicable when the trajectories connected by the knot under consideration may enter other knots. As a matter of principle, one assumes that the system under consideration is finite, and it is surrounded by a “clean” material where trajectories are infinite lines without knots. Then, one solves the problem for the knots on the boundary and moves inwards towards the knot of interest. In the one-dimensional topology of the tree with only one path connecting any two knots, the procedure is unique.

A. 2×2 case

The most simple case is when the knot mixes two incoming and to two outgoing trajectories ($N = 2$) as e.g. in case of specular reflection on an interface. The unitary S-matrix coupling 1 and 2 incoming trajectories to $1'$ and $2'$ outgoing ones (see Fig.5), may be taken in the form

$$S = \begin{pmatrix} r & s \\ -s^* & r^* \end{pmatrix}, |r|^2 = R, |s|^2 = T, R + T = 1. \quad (5.6)$$

Here, r and s are the amplitude of the process $1 \rightarrow 1' 2 \rightarrow 1'$, respectively.

Presenting the wave function on each of the trajectories at the knot as

$$\psi_{1(2)} = \begin{pmatrix} a_{1(2)} \\ 1 \end{pmatrix}, \quad \psi_{1'(2')} = \begin{pmatrix} 1 \\ b_{1'(2')} \end{pmatrix},$$

the matching condition in Eq.(5.5) gives the following relation between the parameters

$$R(1 - a_1 b_{1'}) (1 - a_2 b_{2'}) + T(1 - a_1 b_{2'}) (1 - a_2 b_{1'}) = 0, \quad (5.7)$$

which serves as the boundary condition for Eq.(2.6) or Riccati equation Eq.(2.23).

The usage of it has been explained in Section V. Reiterating, the parameters $a_{1,2}$ ($b_{1',2'}$) in Eq.(5.7) are found from the regular solutions to Eq.(2.6) or Eq.(2.23). They are *independent* from each other and the properties of the knot. The actual meaning of Eq.(5.7) is that when it is resolved relative to $a_{1,2}$ ($b_{1',2'}$) the inverse value gives the initial condition $b_{1,2}(x = 0)$ ($a_{1',2'}(0)$) *i.e.*

$$b_1(0) = \frac{R(1 - a_2 b_{2'}) b_{1'} + T(1 - a_2 b_{1'}) b_{2'}}{R(1 - a_2 b_{2'}) + T(1 - a_2 b_{1'})}, \quad (5.8)$$

$$a_{1'}(0) = \frac{R(1 - a_2 b_{2'}) a_1 + T(1 - a_1 b_{2'}) a_2}{R(1 - a_2 b_{2'}) + T(1 - a_1 b_{2'})}, \quad (5.9)$$

and the expressions for b_2 and $a_{2'}$ obtained by the substitution $1 \leftrightarrow 2$.

B. Transfer matrix

Sometimes it is convenient to consider a pair of trajectories, tag them to 1 and 1', as pieces of a single trajectory (see Fig.6). We assign $x < 0$ to the path 1 and $x > 0$ to 1'. Then Eq.(2.6) is valid for any x excepting the knot point $x = 0$. The knot at the trajectory $1' \leftarrow 1$ is included via the 2×2 transfer matrix $\mathcal{M}_{1' \leftarrow 1}$:

$$\phi(x = +0) = \mathcal{M}_{1' \leftarrow 1} \phi(x = -0), \quad \bar{\phi}(x = +0) = \bar{\phi}(x = -0) \hat{\mathcal{M}}_{1' \leftarrow 1}^{-1} \quad (5.10)$$

as explained in detail in Appendix Sect. E. The transfer matrix is found from the requirements that (i) the matching conditions in Eq.(3.1) are satisfied; (ii) waves on the trajectories other than 1 and 1' are regular.

Denote $\phi_+(x > 0)$ ($\phi_-(x < 0)$) the solution to Eq.(2.6) regular at $+\infty$ ($-\infty$) as in Eq.(2.10). The transfer matrix allows one to continue the solutions across the knot:

$$\bar{\phi}_-(+0) = \bar{\phi}_-(-0) \mathcal{M}_{1' \leftarrow 1}^{-1}, \quad \phi_+(-0) = \mathcal{M}_{1' \leftarrow 1}^{-1} \phi_+(+0) \quad (5.11)$$

In accordance with Eqs.(2.21), and (2.14), the 1-point Green's function $\hat{g}_{1'}^R$ on the trajectory 1' at the knot can be found as

$$\frac{1}{2} (1 + \hat{g}_{1'}^R) = \frac{\phi_+(+0) \bar{\phi}_-(+0)}{\bar{\phi}_-(-0) \phi_+(+0)}.$$

Applying Eq.(5.11), one gets from here that

$$\frac{1}{2} (1 + \hat{g}_{1'}^R) = \frac{\phi_+(+0) \bar{\phi}_-(-0) \mathcal{M}_{1' \leftarrow 1}^{-1}}{\bar{\phi}_-(-0) \mathcal{M}_{1' \leftarrow 1}^{-1} \phi_+(+0)}.$$

Similarly, for the trajectory 1

$$\frac{1}{2} (1 + \hat{g}_1^R) = \frac{\mathcal{M}_{1' \leftarrow 1}^{-1} \phi_+(+0) \bar{\phi}_-(-0)}{\bar{\phi}_-(-0) \mathcal{M}_{1' \leftarrow 1}^{-1} \phi_+(+0)}$$

From here $\hat{g}_{1'}^R \mathcal{M}_{1' \leftarrow 1} = \mathcal{M}_{1' \leftarrow 1} \hat{g}_1^R$ or

$$\hat{g}_{1'}^R = \mathcal{M}_{1' \leftarrow 1} \hat{g}_1^R \mathcal{M}_{1' \leftarrow 1}^{-1} \quad (5.12)$$

For an arbitrary interface, this relation gives the boundary condition for the quasiclassical 1-point Green's function. With the help of Eq.(E1) or Eq.(E2), the transfer matrix \mathcal{M} is generally expressed via the Green's function on the other trajectories coupled by the knot. In the next Section VB 1, we the explicit expression for the transfer matrix is presented for the simplest case of 2 in- and 2-out channels.

1. 2x2 case

In the most important case of a 2×2 knot Fig.5 (e.g. a specular interface), the transfer matrix can be found usual the general formula derived in Sect.E. A more simple way is to make the derivation from the scratch in a specially selected basis (see Sect.E 0 a, for details).

For the knot with the S-matrix in Eq.(5.6), the transfer matrix Eq.(E5) and its inverse read

$$\mathcal{M}_{1' \leftarrow 1} = \frac{(1+R)}{2r^*} \left(1 - \frac{T}{1+R} \hat{g}_{2' \bullet 2} \right), \quad (5.13)$$

$$\mathcal{M}_{1' \leftarrow 1}^{-1} = \frac{(1+R)}{2r} \left(1 + \frac{T}{1+R} \hat{g}_{2' \bullet 2} \right), \quad (5.14)$$

where $\hat{g}_{2' \bullet 2}$ is the normalized ($\hat{g}_{2' \bullet 2}^2 = 1$) “across-knot” Green’s function. It can be presented in different forms.

Its matrix structure is most transparent when $\hat{g}_{2' \bullet 2}$ is written in a factorized form as

$$\frac{1}{2} (1 + \hat{g}_{2' \bullet 2}) = \frac{1}{N} \phi_{2',+} \bar{\phi}_{2,-}, \quad N = \bar{\phi}_{2,-} \phi_{2',+} \quad (5.15)$$

where $\phi_{2',+}$ and $\phi_{2,-}$ are the functions introduced in Sect.IIA taken at the point adjacent to the knot on the trajectory 2’ or 2. They do not depend on the knot parameters R and T . One may think of $\hat{g}_{2' \bullet 2}$ as a 1-point Green’s function on the virtual trajectory built of the pieces 2 and 2’.

From Eqs.(5.15) and (2.13), one concludes that $(1 + \hat{g}_{2' \bullet 2}) \propto (1 + \hat{g}_{2'}^R)(1 + \hat{g}_2^R)$. Eq.(5.15) can be written in terms of the Andreev amplitudes Eq.(2.16), as

$$\frac{1}{2} (1 + \hat{g}_{2' \bullet 2}) = \frac{1}{1 - a_2 b_{2'}} \begin{pmatrix} 1 \\ b_{2'} \end{pmatrix} (1, -a_2)$$

or

$$\hat{g}_{2' \bullet 2} = \frac{1}{1 - a_2 b_{2'}} \begin{pmatrix} 1 + a_2 b_{2'} & -2a_2 \\ 2b_{2'} & -(1 + a_2 b_{2'}) \end{pmatrix}. \quad (5.16)$$

The “across interface” Green’s function can also be written as

$$\hat{g}_{2' \bullet 2} = \frac{1}{1 + \frac{1}{2} [\hat{g}_{2'}, \hat{g}_2]_+} \left(\hat{g}_{2'} + \hat{g}_2 + \frac{1}{2} [\hat{g}_{2'}, \hat{g}_2]_- \right), \quad (5.17)$$

where $\hat{g}_{2,2'}$ are the knot values of the usual 1-point Green’s function on the trajectory 2 and 2’. One should realize that unlike ϕ_{\pm} in Eq.(5.15) and a, b' in Eq.(5.16), both \hat{g}_2 and $\hat{g}_{2'}$ are modified by the knot scattering, and only their combination $\hat{g}_{2' \bullet 2}$ is knot independent.

Using the transfer matrix approach, one can derive the boundary condition to the Riccati equation on the N=2 knot. Most easily this can be done using the transfer matrix in Eq.(E4). Same the result one can get from Eq.(5.7).

We have just presented the boundary condition for the Green’s function on an interface which mixes 2 in-coming and 2 out-going trajectories (e.g. for a specular interface): the Green’s functions on the interface are linearly related by Eq.(5.12) (and the analogous relation for the channel 2 and 2’) where the transfer matrix \mathcal{M} and \mathcal{M}^{-1} can be found from Eqs.(5.13), (5.14) and (5.17). Using these relations, one is able to re-derive Zaitsev’s boundary conditions [6] for a specular reflecting interface.

VI. MULTILAYER SYSTEMS

The purpose of this section is to show the usage of the general theory in practical calculations. First we consider simplest geometry that is a layer deposited on the flat surface of a bulk material with a partially transparent interface. Together with the totally reflecting outer surface, there are two coherently reflecting planes. The other geometry is a system of two layers of arbitrary thickness in contact, in which there are three reflecting planes and rather complicated picture of multiple scattering.

Since our main intention is demonstrate how to use the general formula, we allow ourselves not to worry about the self-consistency of the pair potential. For simplicity, we consider the ballistic case $\Sigma_{imp} = 0$, and the pair potentials in the left (l) and right (r) regions are taken constants Δ_l and Δ_r .

A. A film

The tree-like trajectory near the interface between a layer of thickness d_r and semi-infinite space is shown in Fig.7(a). To build the tree, one considers a particle coming along the path (at the angle θ) marked in Fig.7 by “1” which denote both the location and direction. Due to the partial reflection, a wave on the trajectory “4” is generated. The waves on the paths “2” and “3” are generated due to transmission. The paths “2” and “3” are the semi-infinite, whereas the trajectory “4” comes to the interface again as “5” (the total reflection does not interrupt motion in between “4” and “5”). Again, waves on “6” and “7” are generated, and the path continues towards “9” *etc..* The topological structure of the tree-like trajectory is presented in Fig.7(b).

To find two-point Green’s function $\hat{g}^R(x_1, x_2)$, one solves Eq.(2.3) where the coordinates $x_{1,2}$ correspond now to the points on the tree Fig. 7(b) with the understanding that the tree coordinate x includes information about both the position and direction of the momentum. Due to the one-dimensional topology of the tree, the method described in Sect.II is directly applicable. As before, the 1-point Green’s function $\hat{g}^R(x)$ is given by Eq.(2.19).

The matrix \hat{H}^R in Eq.(2.3) is either

$$\hat{H}_l^R = \begin{pmatrix} \varepsilon + i\delta & \Delta_l \\ -\Delta_l^* & -\varepsilon - i\delta \end{pmatrix} \text{ or } \hat{H}_r^R = \begin{pmatrix} \varepsilon + i\delta & \Delta_r \\ -\Delta_r^* & -\varepsilon - i\delta \end{pmatrix}$$

for the tree coordinate x in the left or right regions. For future references, the free bulk 1-point Green’s function in the left (right) region $\hat{g}_{0,l(r)}^R$ equals

$$\hat{g}_{0,l(r)}^R = \frac{1}{\xi_{l(r)}^R} \hat{H}_{r(l)}^R$$

where $\xi_{l(r)}^R = \sqrt{(\varepsilon + i\delta)^2 - |\Delta_{l(r)}|^2}$, $\Im \xi_{l(r)}^R > 0$.

Considered as a function of x_1 , $\hat{g}^R(x_1, x_2)$ has a source at $x_1 = x_2$ which generates waves propagating away from x_2 . The regularity condition requires that the waves decay when propagating from the source to branches of the tree. The propagation in between the knots is described by Eqs.(2.6), or (2.8), and the knots are incorporated by the matching conditions in Eq.(3.1) or their more advanced version in Eqs.(5.5), or (5.10).

Let us first find 1-point Green's function at the tree point x in between "4" and "5". In accordance with Sect.II, one has to find solutions ϕ_+ which describes the wave spreading from the point x in the positive direction, and ϕ_- propagating in the opposite direction. In the present example, the wave ϕ_+ spreads to the paths "5", "6", "7", "8"..., and ϕ_- spreads to "4", "3", "2", "1".... We chose to think that the particle moves along the "root" path "1" → "4" → "5" → "8" → "9"..., and exclude the "side" branches "2", "3", "6", "7", ... using the transfer matrix approach (see Eq.(5.11)).

Take e.g. the knot where the trajectories "1-4" meet (see Fig.7(a)). The transfer matrix $\mathcal{M}_{4 \leftarrow 1}$ can be expressed in accordance with Eq.(5.13) via the "across-knot" Green's function $\hat{g}_{3 \bullet 2}$. In the present simple case, when "2" and "3" extend to infinity and \hat{H}^R is same for "2" and "3", one can conclude from Eq.(5.15) or Eq.(5.16) that $\hat{g}_{3 \bullet 2} = \hat{g}_{0,l}^R$, where $\hat{g}_{0,l}^R$ is the bulk Green's function in the left region. For any of the identical knots, the transfer matrix reads

$$\mathcal{M} = \frac{(1+R)}{2r^*} \left(1 - \frac{T}{1+R} \hat{g}_{0,l}^R \right)$$

where $R = |r|^2$ and $T = 1 - R$ are the interface reflection and transmission probabilities.

The functions $\phi_{\pm}(x)$ on the root trajectory, where x is the coordinate along the root counted from a knot, are found with the help of Eq.(2.6) supplemented with the boundary condition connecting the 2-component amplitude leaving the knot ϕ_{out} ($out = "4", "8", "12", \dots$) via the incoming wave ϕ_{in} ($in = "1", "5", "9", \dots$)

$$\phi_{out} = \mathcal{M} \phi_{in}.$$

In the present case, when the free motion on the root trajectory is perturbed by the equidistant knots, one can use the method developed in Sect.B for periodic potentials. The period of the structure is $2D_\theta$, $D_\theta = d_r / \cos \theta$ where θ is the angle between the direction of the momentum and the perpendicular to the interface.

The functions $\phi_{\pm}(x)$ are eigenfunctions of the evolution operator $\hat{U}_{2D_\theta}(x)$ generating the translation by the period $x \rightarrow x + 2D_\theta$ (see Sect.B). The free evolution operator $\hat{U}^{(r)}(x + x_0, x_0)$ in the right region is

$$\hat{U}^{(r)}(x + x_0, x_0) = e^{\frac{i}{v} \hat{H}_r^R x} = \cos\left(\frac{\xi_r^R x}{v}\right) + i \hat{g}_{0,r}^R \sin\left(\frac{\xi_r^R x}{v}\right),$$

$\hat{g}_{0,r}^R$ being the bulk Green's function.

The full evolution operator $\hat{U}_{2D_\theta}(x)$ reads

$$\hat{U}_0(x) = A \exp\left(\frac{i \xi_r^R}{v} \hat{g}_{0,r}^R x\right) \left(1 - \frac{T}{1+R} \hat{g}_{0,l}^R \right) \exp\left(\frac{i \xi_r^R}{v} \hat{g}_{0,r}^R (2D_\theta - x)\right),$$

where $A = \frac{(1+R)}{2r^*}$. Finding the two eigenfunctions of this matrix, one knows $\phi_{\pm}(x)$ and, therefore, the full 2-point Green's function from Eq.(2.12).

As explained in Sect.B, the 1-point Green's function can be extracted from $\hat{U}_{2D_\theta}(x)$ by purely algebraic transformations. The Green's function for the direction of the momentum $(\mathbf{p})_z = p_F \cos \theta$ at the distance from the interface z ($z > 0$ in the right region) reads from Eq.(2.27)

$$\hat{g}^R(z, \theta) = \mathcal{F}_R \left[\exp \left(\frac{i\xi_r^R}{v} \hat{g}_{0,r}^R x \right) \left(1 - \frac{T}{1+R} \hat{g}_{0,l}^R \right) \exp \left(\frac{i\xi_r^R}{v} \hat{g}_{0,r}^R (2D_\theta - x) \right) \right] \Big|_{x=\frac{z}{\cos \theta}} \quad (6.1)$$

where the “formatting” operation $\mathcal{F}_R [\dots]$ is defined in Eq.(2.27). The “formatting” can be performed analytically but the result looks rather awkward and hardly any information can be extracted from it without a computer. On the other hand, the “formatting” operation is easily implemented numerically, and for this reason we leave as final the expression for Green’s function in Eq.(6.1).

Consider now the left region and the knot “1”- “4” in Fig.7(a). The left region Green’s functions are those on trajectories “2” and “3”. To apply formula in Sect. E and one should substitute 1 for “2” and 1’ for “3”. Since trajectories “2” and “3” are semi-infinite, the combination $\phi_+(+0)\bar{\phi}_-(-0)$ is proportional to the bulk value $(1 + \hat{g}_{0,l}^R)$. The transfer matrix $\mathcal{M}_{4 \leftarrow 1}$ contains the across-knot Green’s function $\hat{g}_{4 \bullet 1}$ analogously to Eq.(5.17). It is easy to see that $\hat{g}_{4 \bullet 1}$ equals to just found $\hat{g}^R(z = +0, \theta)$. Therefore, the Green’s function on the left side of the interface is

$$\hat{g}^R(z = -0, \theta) = \mathcal{F}_R \left[(1 + \hat{g}_{0,l}^R) \left(1 + \frac{T}{1+R} \hat{g}^R(z = +0, \theta) \right) \right]$$

At other points in the left region ($z < 0$), the Green’s function is found with the help of the free evolution operator,

$$\hat{g}^R(z, \theta) = \exp \left(\frac{i\xi_l^R}{v} \hat{g}_{0,l}^R x \right) \hat{g}^R(z = -0, \theta) \exp \left(-\frac{i\xi_l^R}{v} \hat{g}_{0,l}^R x \right) \Big|_{x=|z/\cos \theta|} \quad (6.2)$$

In Fig.8, we show the density of states on the film side of the interface, *i.e.* $\Im \hat{g}^R(z = +0, \theta)$ Eq.(6.1), for $D_\theta = v/|\Delta_l|$ and the pair potential in the left and right parts of different signs, $\Delta_l = -\Delta_r$; the curves parameters differ in the reflectivity R increasing from zero in Fig.8(a) to $R=0.9$ in Fig.8(d).

When $R = 0$, one sees in Fig.8(a) two (zero width) peaks in the gap region $|\varepsilon| < |\Delta|$. The peaks are due to the bound states well-known known in the theory of anisotropic superconductors [34] (see also Sect.IV B). The $\varepsilon = 0$ bound states exist near the trajectory point where the phase of Δ changes abruptly by π . When the thickness d_r is finite, the levels are at a finite energy [26] due to the overlap of the wave functions (e.g. of the states on the “2”-“4” and “5”-“7” paths in Fig. 7(a)) and the level repulsion. The overlap of the separated in space levels and, therefore, the level splitting are exponentially small when D_θ is large.

When R is finite, the splitting increases. First, the reflection gives rise to the on-knot overlap of the levels belonging to the the same knot, e.g. the “2”-“4” and “1”- “3” levels”. By this mechanism, the level is split to $\pm\sqrt{R}|\Delta|$ (cf. Eq.(4.14)). Second, the on-knot overlap in combination with the next neighbour overlap discussed earlier, mixes together all the bound states and transforms the discreet levels into bands. This behaviour is clearly seen in Fig.8(b)-(d).

B. Sandwich

In this Section we consider a more general case when the left region is a finite layer of thickness d_l . As previously, the order parameter is assumed to be constant in the layers.

The typical tree-like trajectory formed by multiple reflections on the outer surfaces and the interface, is shown in Fig.9(a). As in Fig.7, the numbers tag the coordinate on the trajectory. Topological structure of (a fragment of) the tree is shown in Fig.9(b); the tagging in same is in Fig.9(a). The centre of the tree is (arbitrarily) chosen at the “5”-“8” knot; the tree structure looks same if viewed from different knots. The pieces of the tree with the arrows in the horizontal direction correspond to the the left layer, and points on the vertical lines belong to the right layer. Generally, the tree-like trajectory covers (almost) all space but remains nevertheless topologically one-dimensional: The features discussed before are clearly seen here that is (i) if a line of the tree is cut, two disconnected pieces are produced or, equivalently, (ii) there is no closed loops on the tree.

First we calculate the knot values of the Green’s functions, for the central knot “5”-“8”. Other knots are equivalent to the central knot. On both horizontal and vertical branches in Fig. 9, the arrays of knots are periodical, separated by $2D_{l,\theta}$, $D_{l,\theta} = d_l / \cos \theta$ for the horizontal branches (the left layer) and $2D_{r,\theta}$, $D_{r,\theta} = d_r / \cos \theta$, on the vertical branches (the right layer).

As in the previous section (see Sect. B for prove), the 1-point Green’s function at “5”, \hat{g}_5^R , is simply related to the evolution operator $\hat{U}_{9 \leftarrow 5}$ advancing the wave function at “5” to the periodically equivalent point “9” (see Fig. 9(b)). Crossing the knot from “5” to “8” with the help of the transfer matrix, \mathcal{M}_\downarrow , build analogously to Eq.(5.13),

$$\mathcal{M}_\downarrow = \frac{(1+R)}{2r^*} \left(1 - \frac{T}{1+R} \hat{g}_{7 \bullet 6} \right) ,$$

and moving from “8” to “9” by $\exp(2iD_{\theta,r}\hat{g}_{0,r}^R)$, one get $\hat{U}_{9 \leftarrow 5}$ as the ordered product of the two matrices. The same matrices but multiplied in the different order, give the evolution operator $\hat{U}_{8 \leftarrow 3}$ and, therefore \hat{g}_8^R .

Changing notation in Eq.(5.17) and collecting formulae together, one gets

$$\hat{g}_{7 \bullet 6} = \frac{1}{1 + \frac{1}{2}[\hat{g}_7, \hat{g}_6]_+} \left(\hat{g}_7 + \hat{g}_6 + \frac{1}{2}[\hat{g}_7, \hat{g}_6]_- \right) \quad (6.3a)$$

$$\hat{g}_8^R = \mathcal{F}_R \left[\left(1 - \frac{T}{1+R} \hat{g}_{7 \bullet 6} \right) \exp(2iD_{\theta,r}\hat{g}_{0,r}^R/v) \right] \quad (6.3b)$$

$$\hat{g}_5^R = \mathcal{F}_R \left[\exp(2iD_{\theta,r}\hat{g}_{0,r}^R/v) \left(1 - \frac{T}{1+R} \hat{g}_{7 \bullet 6} \right) \right] . \quad (6.3c)$$

These equations allow one to find the knot values of the Green’s function in the right region via the left region counterparts.

In the same way one can derive expressions where $\hat{g}_{6,7}^R$ are related to $\hat{g}_{5,8}^R$

$$\hat{g}_{8 \bullet 5} = \frac{1}{1 + \frac{1}{2}[\hat{g}_8, \hat{g}_5]_+} \left(\hat{g}_8 + \hat{g}_5 + \frac{1}{2}[\hat{g}_8, \hat{g}_5]_- \right) \quad (6.4a)$$

$$\hat{g}_7^R = \mathcal{F}_R \left[\left(1 - \frac{T}{1+R} \hat{g}_{8\bullet 6} \right) \exp(2iD_{\theta,l}\hat{g}_{0,l}^R/v) \right] \quad (6.4b)$$

$$\hat{g}_6^R = \mathcal{F}_R \left[\exp(2iD_{\theta,l}\hat{g}_{0,l}^R/v) \left(1 - \frac{T}{1+R} \hat{g}_{8\bullet 5} \right) \right]. \quad (6.4c)$$

Eqs.(6.3) and (6.4) allow one to find iteratively the knot values of the Green's function. Unless the reflection R is too small, the iterations converge rather fast. For almost transparent interfaces, $R \ll 1$, a slightly different procedure is more efficient: as the periods, one chooses the paths like “4” → “5” → “7” → “14” → “16”.

Given the knot values, the Green's function at other points can be calculated by formulae analogous to Eq.(6.2).

Fig.10 shows the trajectory resolved density of states at the interface, $\Im \hat{g}_{z=0,\theta}^R$ for the case when the $\Delta_l = -\Delta_r$ and the layers of equal thickness $D_{l,\theta} = D_{r,\theta} = v/|\Delta_l|$.

As expected, the sandwich with a transparent interface, $R = 0$, has a considerable spectral weight at low energies which is represented by the band centred at $\varepsilon = 0$ (see Fig.10(a)). The overall picture is very different from the BCS density of states: the spectrum is given by well-defined bands with strong edge singularities. As in case of a film, the reflection splits the $\varepsilon = 0$ bound states, and the bands move towards higher energies. When the reflectivity is as low as 0.1 (see Fig.10(b)), there is no states at, and in the vicinity of $\varepsilon = 0$. The forbidden bands become more narrow, and the edge singularities become smoother. From Fig.10(c) and (d), one sees that for $R \gtrsim 0.5$ the states are pushed to the energies $\gtrsim \Delta$.

In the next section, we use these results to evaluate the “superfluid density”, an observable sensitive to the shape of the density of states.

1. Superfluid density

In this section we calculate ρ_s , a parameter which controls the current density \mathbf{j} induced by a weak spatially homogeneous static vector potential, \mathbf{A} ,

$$\mathbf{j} = -\rho_s \frac{c}{4\pi} \frac{1}{\lambda_L^2} \mathbf{A},$$

λ_L being the (bulk) London penetration depth at zero temperature. In the two-fluid lexicon, ρ_s is the “superfluid density” or the “fraction of superconducting electrons”.

In the present case of a two-layer system, the local current induced by in-plane homogeneous vector potential is z -dependent, being proportional to the local density of states. The total current through the layers is proportional to the average,

$$\rho_s = \frac{1}{d_l + d_r} \int_{-d_l}^{d_r} dz \rho_s(z) , \quad \rho_s(z) = 1 - \int_{-\infty}^{\infty} d\varepsilon \left(-\frac{\partial f_0}{\partial \varepsilon} \right) \nu(\varepsilon, z) \quad (6.5)$$

where f_0 is the Fermi function, and $\nu(\varepsilon, z)$ is the local density of states,

$$\nu(\varepsilon, z) = \text{Re} \int \frac{d\Omega_n}{4\pi} (\hat{g}^R(\varepsilon, \mathbf{n}, z))_{11} .$$

The averaged superfluid density ρ_s in Eq.(6.5) is conveniently written as

$$\rho_s = 1 - \int_{-\infty}^{\infty} d\varepsilon \left(-\frac{\partial f_0}{\partial \varepsilon} \right) \bar{\nu}(\varepsilon) , \quad \bar{\nu}(\varepsilon) \equiv \frac{d_l \bar{\nu}_l(\varepsilon) + d_r \bar{\nu}_r(\varepsilon)}{d_l + d_r} \quad (6.6)$$

where $\bar{\nu}_{l,r}(\varepsilon)$ is the averaged density of states in the left (l) and right (r) layers.

To calculate $\bar{\nu}_{l,r}(\varepsilon)$, one finds the Green's function, as explained in the previous section, and perform integrations with respect to the coordinate z and the direction \mathbf{n} . The spatial dependence, found from the knot values by formulae analogous to Eq.(6.2), is simple and the z -integration can be done analytically. The averaged density of states in the right region reads

$$\begin{aligned} \bar{\nu}_r(\varepsilon) = & \frac{1}{2} \text{Sp} \tau_z \Re \int_0^1 d\mu \left(\hat{g}_{0,r}^R [\hat{g}_{0,r}^R, \hat{g}_5^R]_+ \right. \\ & \left. + \frac{\sin 2\gamma}{2\gamma} \hat{g}_{0,r}^R [\hat{g}_{0,r}^R, \hat{g}_5^R]_- + i \left(\frac{1 - \cos 2\gamma}{2\gamma} \right) [\hat{g}_{0,r}^R, \hat{g}_5^R]_- \right)_{\varepsilon, \mu} \end{aligned} \quad (6.7)$$

where, $\mu = \cos \theta$, $\gamma_{\varepsilon, \mu} \equiv 2d_r \xi_r^R / \mu v$, $\hat{g}_{0,r}^R$ is the bulk Green's function, and \hat{g}_5^R is the knot value of the Green's function on the tree corresponding to the angle θ (see previous Section). After the substitution, $r \rightarrow l$ and $\hat{g}_5^R \rightarrow \hat{g}_6^R$, Eq.(6.7) gives $\bar{\nu}_l$.

The integration with respect to μ in Eq.(6.7) and ε in Eq.(6.6) can be performed only numerically. The integration in Eq.(6.6) along the real ε axes may be slowly converging due to the band edge singularities; for better convergence, one may integrate along line $\Im \varepsilon = i \frac{T\pi}{2}$ or transform the integral to the Matsubara sum.

We evaluated numerically the superfluid density for a sandwich with equal thickness of the layers $d_{l,r} = v/|\Delta_{l,r}|$ and the π differences in the order parameter phase $\Delta_l = -\Delta_r$. In Fig.11, the superfluid density as a function of temperature is shown for different reflectivity R .

The curve for $R = 0$ shows large negative ρ_s at low temperatures which would lead to amplification of the applied magnetic field rather than the Meissner screening. This feature is due to the large low energy spectral weight seen in Fig.10(a). Therefore, our data support the recent idea put forward by Fauchere, Belzig, and Blatter [26] about the paramagnetic instability near the surface where the order parameter changes its sign. However, one sees in Fig.10 that the effect is very sensitive to the presence of the partially reflective interface: reflection with the probability as low as 4 percent makes ρ_s positive at any temperature.

VII. CONCLUSIONS

In this paper we have reconsidered the part of the quasiclassical theory of superconductivity which concerns interfaces between superconductors (SIS) or a normal metal and a superconductors (NIS). Since the interface violates the condition of applicability of the quasiclassical approximation, the reflection and transmission processes must be included via a boundary condition. In the approach taken in the paper, the master boundary condition in Eq.(3.1) is formulated for the effective wave functions factorizing the 2-point Green's

function. In the boundary condition, the two-component amplitudes in N in-coming and N out-going channels are related to each other via the S-matrix. The latter is sensitive to microscopic details of the interface and is considered as an input in the quasiclassical theory. The theory is equally applicable to specular interfaces ($N = 2$), as well as to the many channel case which models a rough surface or interface. In Sections IV, V, and VB, the master boundary condition is reformulated in various forms, suitable for the one or the other application.

In Sect.IV, we have presented a general solution to the ballistic problem of the scattering of electron-and hole-like *excitation*. This result extends the theory of the NIS interface [20] to the many channel situation; SIS case is also included. As in Ref. [20], the solution is general in the sense that it expresses the full amplitude of the multiple processes of the Andreev electron \leftrightarrow hole conversion and ordinary scattering via the amplitudes of the elementary processes. By this, the problem is split into independent and more simple problems. The theory of multi-channel bound states is also considered. The formulation which operates with excitations rather than bare particles, is especially convenient for the kinetic theory in the framework of the Boltzmann-type equations, for which it provides the boundary condition for the distribution function of the excitations [11,35].

For a general case *i.e.* when the disorder and inelastic collisions are allowed, the boundary value of the 2-component wave functions $\phi = \begin{pmatrix} u \\ v \end{pmatrix}$ factorizing the trajectory Green's function are found in Sect.V. Since the mean field equations are linear, this result can be recast as the boundary condition for the Andreev amplitudes u/v of the Riccati equation approach. In a most compact and symmetric form, the boundary condition is given by Eq.(5.5). For the specular interface, the boundary condition for the Riccati equation is given by Eq.(5.7), or explicitly by Eqs.(5.8), and (5.9).

One more form of the boundary condition is presented in Sect.VB, where the expression for the transfer matrix is derived. The transfer matrix, which couples the wave functions or the 1-point Green's functions on the chosen pair of in- and out-channels, absorbs information about all other $2(N - 1)$ channels. This modification of the boundary condition is convenient when one solves the Eilenberger equations for the 1-point Green's function. In the simplest 2-channel case (specular reflection), this boundary condition reproduces Zaitsev's results [6]. The new form seems to be more flexible and convenient.

For the derivation, we use the technique of the 2-point Green's function. In our opinion, the technique provides an adequate language to discuss the semiclassical physics in superconductors which we qualitatively considered in Section I. The 2-point Green's function gives a full description of the coherent propagation of electron and hole along a common classical path. In spite of the fact that observables can be expressed via the 1-point Green's function only, the language of the quasiclassical 2-point Green's function is not redundant: Offering a physically transparent formalism, it is free from some uniqueness problems which plague the standard “ ξ -integrated” formulation. Note also that with all possible simplifications already done, the quasiclassical 2-point Green's function obeys Eqs.(2.2), and (2.3) which, unlike the Eilenberger equations, have a familiar form of an equation for a propagator. Therefore, one may directly apply the intuition and experience gained in other fields of the quantum theory.

Another attractive feature of the 2-point Green's function technique is that it allows one to define effective wave functions. The latter factorize the Green's function averaged

with respect to disorder or phonons. Although these “wave functions” have usual quantum mechanical meaning only in ballistic case, it seems to be advantageous that one may use the unified language of trajectories and wave functions discussing both the ballistic motion and the propagation in the presence of disorder or inelastic collisions.

The effective wave function, $\phi = \begin{pmatrix} u \\ v \end{pmatrix}$ obeys the linear Andreev-type equation Eq.(2.6). There is a variety of methods one can chose to solve the system of two linear differential equations for u and v . One of them is to derive the equation for the ratio u/v which turns out to be the Riccati equation suggested in [24,25]. As the logarithmic derivative ψ'/ψ in the usual Schrödinger equation does, the choice of the ratio u/v has the indisputable practical advantage which is due to insensitivity of the ratio to the normalisation of ϕ . The Riccati equation approach which has proven to be very convenient and efficient for numerics, finds rather natural physical interpretation in the 2-point Green’s function technique of the present paper. (For the latest development of the Riccati equation approach including the interface boundary condition see e-preprint of M. Eschrig [37].)

An important part of this paper is the understanding that the classical trajectory transforms to a topologically 1-dimensional simply connected tree in the case of many interfaces and/or boundaries. The extended arguments in favour of this point of view have been presented in Section I. Although, this assertion may look wrong in simple idealized geometries, like e.g., a sandwich with strictly parallel outer and the interface planes Fig.2, we argue that small deviations from the perfection eliminate accidental crossings of trajectories (as in non-integrable billiards). In our opinion, the difficulties with the quasiclassical theory encountered in [7,8] are due to the fact that some interference contributions survive the procedure of the integration with respect to the layer thickness: Indeed, rigid variations of the layer thickness do not eliminate all the loops. We believe that some roughness, larger then the Fermi wave length but small and invisible on the quasiclassical scale, will restore the quasiclassical results.

To show the new theory in action, we solve in Sect.VI two simple problems: (i) a film separated from a bulk material by a partially transparent interface; (ii) a two layer system with arbitrary transparent interface. (The latter was classified in [8] as quasiclassically unsolvable.) Motivated by recent ideas about the origin of the paramagnetic effect [36], we evaluate the density of states and the superfluid density when the phase of the order parameters in the layers differs in π , a scenario of paramagnetic instability suggested in [26]. Our results confirm the very possibility that the superfluid density ρ_s may be negative (Meissner “anti-screening”) but we observe also that ρ_s is strongly affected by reflection on the interface: when the probability of the reflection $R > 0.04$, the Meissner *screening* is restored. The implications of these results for a realistic theory of the paramagnetic instability requires further studies.

ACKNOWLEDGMENTS

We are thankful to W. Belzig and C. Bruder for discussions, and to D. Rainer for very useful comments. This study begun during the stay of one of us (A.S) at the Institut für Theorie der Kondensierten Materie, Universität Karlsruhe, and A.S. would like to thank all the stuff for hospitality and der Deutschen Forschungsgemeinschaft (SFB 195) for support. In part this work was supported by the Swedish Natural Science Research Council.

APPENDIX A: ADVANCED GREEN'S FUNCTIONS

The advanced Green's function $g^A(x_1, x_2)$ is constructed in the same manner as the retarded one: One finds $\phi_{1,2}$ from Eq.(2.6) with \hat{H}^R substitutes for \hat{H}^A and builds the Green's function as in Eqs.(2.12), (2.13) and (2.22).

Combining Eqs.(2.5) and (2.7), one can see that the $\hat{\tau}_x (\phi^R)^*$ with ϕ^R from Eq.(2.6) satisfies the corresponding equation in the A-case. Then, the normalized Eq.(2.11) solutions are related to each other as

$$\phi_+^A = i\hat{\tau}_x (\phi_+^R)^* , \quad \phi_-^A = i\hat{\tau}_x (\phi_-^R)^* . \quad (\text{A1})$$

The Andreev amplitudes a and b Eq.(2.16) are related now as

$$a^A = 1/ (a^R)^* , \quad b^A = 1/ (b^R)^* ,$$

and Green's functions as

$$\hat{g}^R(x_1, x_2) = \hat{\tau}_x \hat{g}^{A*}(x_1, x_2) \hat{\tau}_x$$

For future references, the symmetry in the 1-point Green's functions is given by the following well-known relations ($\boldsymbol{\varepsilon} = (\varepsilon, \mathbf{n})$, $\boldsymbol{\varepsilon}^* = (\varepsilon^*, \mathbf{n})$)

$$\hat{g}_{\boldsymbol{\varepsilon}}^R(\mathbf{r}) = -\hat{\tau}_z (\hat{g}_{\boldsymbol{\varepsilon}^*}^A(\mathbf{r}))^\dagger \hat{\tau}_z , \quad \hat{g}_{\boldsymbol{\varepsilon}}^R(\mathbf{r}) = (\hat{g}_{-\boldsymbol{\varepsilon}^*}^R(\mathbf{r}))^\dagger$$

The first of them follows from Eq.(A1), and the second one reflects the symmetry $\hat{H}_{\boldsymbol{\varepsilon}}^R = -\hat{\tau}_z \hat{H}_{-\boldsymbol{\varepsilon}}^A \hat{\tau}_z$.

APPENDIX B: EVOLUTION IN PERIODIC POTENTIAL

To prove validity of Eq.(2.26), one first solves the 2×2 eigenvalue problem

$$\hat{U}_L(x)\psi(x) = \gamma\psi(x) .$$

and finds the eigenfunctions $\psi_{1,2}$ (with x as a parameter) and the eigenvalues $\gamma_{1,2}$. It follows from the conservation of normalization in Eq.(2.9) that $\text{Det } U = 1$, and, therefore,

$$\gamma_1 \gamma_2 = 1 .$$

Denote γ_1 the eigenvalue for which $|\gamma_1| < 1$, ¹ and normalize the eigenfunctions to satisfy $\bar{\psi}_2 \psi_1 = 1$. It is clear now, that $\psi_1(x)$ continued along the trajectory with the help of the evolution matrix $\hat{U}_L(x)$ gives the solution denoted in Eq.(2.10) as $\phi_+(x)$: Indeed, it satisfies Eq.(2.6) and decays at $x \rightarrow \infty$ as $\gamma_1^{x/L}$. By the same argument, $\phi_- = \psi_2$. From Eq.(2.20), the Green function now reads

¹ When considering \hat{g}^R , the variable ε has a finite imaginary part and the matrix \hat{H}^R is not Hermitian. Then, the evolution matrix is not unitary and $|\gamma_{1,2}| \neq 1$.

$$\hat{g}^R = \psi_1 \bar{\psi}_2 + \psi_2 \bar{\psi}_1 .$$

Seeing that the evolution 2×2 matrix can be expanded in its normalized eigenfunctions as

$$\hat{U}_L(x) = \frac{1}{2}(\gamma_1 + \gamma_2)\hat{1} + \frac{1}{2}(\gamma_1 - \gamma_2)(\psi_1 \bar{\psi}_2 + \psi_2 \bar{\psi}_1) ,$$

the traceless part of $\hat{U}_L(x)$ is proportional to \hat{g}^R . The normalization condition fixes the proportionality coefficient, and one comes to Eq.(2.26).

To build the evolution matrix, one may use the following procedure. First consider two fundamental solutions to Eq.(2.6), ψ_I and ψ_{II} , which satisfy the following boundary conditions

$$\psi_I(x) = \begin{pmatrix} 1 \\ 0 \end{pmatrix} , \quad \psi_{II}(x+L) = \begin{pmatrix} 0 \\ 1 \end{pmatrix} .$$

and find $\psi_I(x+L)$ and $\psi_{II}(x)$,

$$\psi_I(x+L) = e^{i\Phi_L(x)} \begin{pmatrix} 1 \\ \alpha_L(x) \end{pmatrix} , \quad \psi_{II}(x) = e^{i\Phi_L(x)} \begin{pmatrix} \beta_L(x) \\ 1 \end{pmatrix} .$$

The exponential factor is same for ψ_I and ψ_{II} as required by the conservation of the normalization in Eq.(2.9). The parameters $\alpha_L(x)$, $\beta_L(x)$, and $\Phi_L(x)$ can be calculated conveniently in the Riccati equation technique.

Denote $\alpha_0(x; x_0)$ solution to Eq.(2.23) with the boundary condition $\alpha_0(x = x_0; x_0) = 0$; then (see Eq.(2.24))

$$\alpha_L(x) = \alpha_0(x+L; x) , \quad \Phi_L(x) = \int_x^{x+L} dx' (\varepsilon^R(x') + \Delta^R(x') \alpha(x'; x))$$

Similarly,

$$\beta_L(x) = \beta_0(x, x+L)$$

where $(\beta_0(x, x_0))^{-1}$ is the solution to Eq.(2.23) with the boundary condition $\beta_0(x = x_0, x_0) = 0$.

Building the evolution matrix from the fundamental solutions, one gets

$$\hat{U}_L(x) = e^{i\Phi_L(x)} \begin{pmatrix} 1 & -\beta_L(x) \\ \alpha_L(x) & e^{-2i\Phi_L(x)} - \alpha_L(x)\beta_L(x) \end{pmatrix}$$

The traceless part of it, $\hat{U}'_L(x)$, reads

$$\hat{U}'_L(x) = \frac{1}{2} e^{i\Phi_L(x)} \begin{pmatrix} 1 - e^{-2i\Phi_L(x)} + \alpha_L(x)\beta_L(x) & -2\beta_L(x) \\ 2\alpha_L(x) & -1 + e^{-2i\Phi_L(x)} - \alpha_L(x)\beta_L(x) \end{pmatrix} .$$

Up to the normalization factor, this matrix is equal to $\hat{g}^R(x)$.

APPENDIX C: FORMAL SOLUTION: I

Here, we analyze some formal linear algebra aspects of the matching conditions in Eq.(3.1).

Generally, the wave functions may be presented in the following form:

$$\psi_{k'} = A_{k'} \begin{pmatrix} 1 \\ \mu_{k'} \end{pmatrix}, \quad \psi_i = B_i \begin{pmatrix} \nu_i \\ 1 \end{pmatrix} \quad (C1)$$

Denote $|X\rangle$ the column with elements X_1, \dots, X_N or $X_{1'}, \dots, X_{N'}$. One obtains from Eqs.(3.1), and (3.2)

$$|A\rangle = \hat{S}\hat{\nu}|B\rangle, \quad |B\rangle = \hat{S}^\dagger\hat{\mu}|A\rangle. \quad (C2)$$

where $\hat{\mu}$ and $\hat{\nu}$ are diagonal matrices $N \times N$ with $(\hat{\mu})_{k'k'} = \mu_{k'}$ and $(\hat{\nu})_{kk} = \nu_k$.

The two equalities in Eq.(C2) are compatible only if

$$\mathcal{D}(\{\nu\}, \{\mu\}) \equiv \det \left| \left| 1 - \hat{S}\hat{\nu}\hat{S}^\dagger\hat{\mu} \right| \right| = 0, \quad (C3)$$

As expected, the parameters μ 's and ν 's are not independent: Eq.(C3) gives a relation among them, which is *linear* in each of the parameters (see Section D), making it possible to express one of the μ 's or ν 's through all others.

For instance, one may give any values to μ 's and ν 's in all channels excepting the l -th incoming one. Then ν_l is fixed by Eq.(C3),

$$\nu_l^{-1} = \langle l | \hat{S}^\dagger\hat{\mu}\hat{S}_l | l \rangle. \quad (C4)$$

where

$$\hat{S}_l = \left(\hat{S}^\dagger - \hat{\nu}^{(l)}\hat{S}^\dagger\hat{\mu} \right)^{-1}, \quad (C5)$$

and $\hat{\nu}^{(l)}$ denotes the matrix which differs from $\hat{\nu}$ only in that the element $(\hat{\nu}^{(l)})_{ll} = 0$; here and below $\langle i | \hat{Q} | j \rangle \equiv Q_{ij}$.

From Eq.(C2) one finds now the coefficients A 's and B 's, they are proportional to one of them, say B_l . It is convenient to put $B_l = C\nu_l^{-1}$. In this way, one gets the solution to the matching conditions in Eq.(3.1) corresponding to the given set of $\mu_{k'}$ and $\nu_{i \neq l}$'s :

$$\psi_l^{(l)} = C \begin{pmatrix} 1 \\ \nu_l^{-1} \end{pmatrix}, \quad \psi_{m \neq l}^{(l)} = C \langle m | \hat{S}^\dagger\hat{\mu}\hat{S}_l | l \rangle \begin{pmatrix} \nu_m \\ 1 \end{pmatrix}, \quad \psi_{k'}^{(l)} = C \langle k' | \hat{S}_l | l \rangle \begin{pmatrix} 1 \\ \mu_{k'} \end{pmatrix}; \quad (C6)$$

here ν_l is given by Eq.(C4), $k, m = 1, \dots, N$, and C is arbitrary.

In the same way one builds the solution where all the μ 's and ν 's are given as input excepting $\mu_{n'}$ adjusted to meet the condition in Eq.(C3):

$$\psi_{n'}^{(n')} = C \begin{pmatrix} \mu_{n'}^{-1} \\ 1 \end{pmatrix}, \quad \psi_{k' \neq l'}^{(n')} = C \langle k' | \hat{S}\hat{\nu}\hat{S}_{n'}^\dagger | n' \rangle \begin{pmatrix} 1 \\ \mu_{k'} \end{pmatrix}, \quad \psi_m^{(n')} = C \langle m | \hat{S}_{n'}^\dagger | n' \rangle \begin{pmatrix} \nu_m \\ 1 \end{pmatrix}; \quad (C7)$$

$k', m = 1, \dots, N$,

$$\mu_{n'}^{-1} = \langle n' | \hat{S}\hat{\nu}\hat{S}_{n'}^\dagger | n' \rangle. \quad (C8)$$

and

$$\hat{S}_{n'}^\dagger = \left(\hat{S} - \hat{\mu}^{(n')} \hat{S}\hat{\nu} \right)^{-1}, \quad (C9)$$

APPENDIX D: FORMAL SOLUTION: II

Transforming $1 - \hat{S}\hat{\nu}\hat{S}^\dagger\hat{\mu} = (1 - \hat{S}\hat{\nu}^{(l)}\hat{S}^\dagger\hat{\mu})\left(1 - \nu^{(l)}\left(\hat{S}^\dagger - \hat{\nu}^{(l)}\hat{S}^\dagger\hat{\mu}\right)^{-1}|l\rangle\langle l|\hat{S}^\dagger\hat{\mu}\right)$, and using identity $\det(1 + |X\rangle\langle Y|) = 1 + \langle Y|X\rangle$, one gets

$$\mathcal{D}(\{\nu\}, \{\mu\}) = \mathcal{D}(\{\nu^{(l)}\}, \{\mu\}) \left(1 - \nu^{(l)}\langle l|\hat{S}^\dagger\hat{\mu}\hat{S}_l|l\rangle\right) \quad (D1)$$

with \hat{S}_l in Eq.(C5), and $\hat{\nu}^{(l)}$ denotes the matrix which differs from $\hat{\nu}$ only in that the element $(\hat{\nu}^{(l)})_{ll} = 0$.

Similarly,

$$\mathcal{D}(\{\nu\}, \{\mu\}) = \mathcal{D}(\{\nu\}, \{\mu^{(n')}\}) \left(1 - \mu^{(n')}\langle n'|\hat{S}\hat{\nu}\hat{S}_{n'}^\dagger|n'\rangle\right)$$

where $\hat{S}_{n'}^\dagger$ is defined in Eq.(C9).

Sometimes calculations become shorter when one changes the representation. Since the S -matrix in the Eq.(3.1) is a scalar in the electron-hole space, the matching condition is unchanged by any rotation $\psi \rightarrow \psi_{\mathcal{O}} = \hat{\mathcal{O}}\psi$,

$$\hat{\mathcal{O}} = \frac{1}{1 - \mu_0\nu_0} \begin{pmatrix} 1 & -\nu_0 \\ -\mu_0 & 1 \end{pmatrix},$$

After the rotation, the basis wave function in Eq.(C1) has the same form with $(\dots) \rightarrow (\dots)_{\mathcal{O}}$

$$\begin{aligned} \mu_{\mathcal{O}k'} &= \frac{\mu_{k'} - \mu_0}{1 - \mu_{k'}\nu_0} \\ \nu_{\mathcal{O}i} &= \frac{\nu_i - \nu_0}{1 - \mu_0\nu_i} \\ A_{\mathcal{O}k'} &= A_{k'} \frac{1 - \mu_{k'}\nu_0}{1 - \mu_0\nu_0} \\ B_{\mathcal{O}i} &= B_i \frac{1 - \mu_0\nu_i}{1 - \mu_0\nu_0} \end{aligned}$$

One sees that by proper rotations any pair $\mu_{k'}, \nu_i$ can be nullified in the intermediate calculations. Of course, all other coefficients will also be changed. Calculations done, one gets to the original basis.

Eqs.(4.8), and (4.9) can be written in a more compact form. From Eq.(D1),

$$\frac{1}{1 - \alpha_{0l}^{(e)}\alpha_l^{(h)}} = \frac{\mathcal{D}_l}{\mathcal{D}_0}$$

where

$$\mathcal{D}_0 = \mathcal{D}(\{\alpha^{(e)}\}, \{\alpha^{(h)}\})$$

and

$$\mathcal{D}_l = \mathcal{D}(\{\alpha^{(e)}\}, \{(\alpha^{(h)})^{(l)}\})$$

Absorbing \mathcal{D}_l into \mathbf{S}_l *i.e.* $\mathbf{S}_l = \mathcal{D}_l \mathbf{S}_l$, and using obvious $|l\rangle \beta^{(e)*} = \hat{\beta}^{(e)*}|l\rangle$ etc., etc the scattering amplitudes read

$$\begin{aligned} B_l^{(l)} &= \frac{1}{\mathcal{D}_0} \left(\langle l | S^\dagger \hat{\alpha}^{(e)} \hat{\mathbf{S}}_l | l \rangle - \mathcal{D}_l \alpha_l^{(e)} \right) \\ B_{k \neq l}^{(l)} &= \frac{1}{\mathcal{D}_0} \langle k | \hat{\beta}^{(h)} S^\dagger \hat{\alpha}^{(e)} \hat{\mathbf{S}}_l \hat{\beta}^{(e)*} | l \rangle \\ A_{k'}^{(l)} &= \frac{1}{\mathcal{D}_0} \langle k' | \hat{\beta}^{(e)} \hat{\mathbf{S}}_l \hat{\beta}^{(e)*} | l \rangle \end{aligned}$$

APPENDIX E: TRANSFER MATRIX

Another possibility for resolving the matching conditions is via the transfer matrix $\hat{\mathcal{M}}_{n' \leftarrow l}$

$$\psi_{n'} = \hat{\mathcal{M}}_{n' \leftarrow l} \psi_l ,$$

which couples the wave functions

$$\psi_l = \begin{pmatrix} u_l \\ v_l \end{pmatrix} , \quad \psi_{n'} = \begin{pmatrix} u_{n'} \\ v_{n'} \end{pmatrix}$$

on a selected pair of trajectories l and n' ; the parameters $\mu_{k' \neq n'}$ and $\nu_{i \neq l}$ are supposed to be given.

As usual, the transfer matrix can be built out of the elements of two particular solutions $\Psi^{I,II}$. Take Ψ^I to be the solution in Eq.(C6) with $\mu_{n'}$ put to zero,

$$\Psi^I : \quad \psi_{n'}^{(I)} = \langle n' | \hat{\mathbf{S}}_{n'l} | l \rangle \begin{pmatrix} 1 \\ 0 \end{pmatrix} , \quad \psi_l^I = \begin{pmatrix} 1 \\ \langle l | \hat{S}^\dagger \hat{\mu}^{(n')} \hat{\mathbf{S}}_{n'l} | l \rangle \end{pmatrix}$$

and Ψ^{II} the solution Eq.(C7) with $\nu_l = 0$,

$$\Psi^{II} : \quad \psi_{n'}^{(I)} = \begin{pmatrix} \langle n' | \hat{S} \hat{\nu}^{(l)} \hat{\mathbf{S}}_{n'l}^+ | n' \rangle \\ 1 \end{pmatrix} , \quad \psi_l^{(II)} = \langle l | \hat{\mathbf{S}}_{n'l}^+ | n' \rangle \begin{pmatrix} 0 \\ 1 \end{pmatrix}$$

where

$$\hat{\mathbf{S}}_{n'l} = \left(\hat{S}^\dagger - \hat{\nu}^{(l)} \hat{S}^\dagger \hat{\mu}^{(n')} \right)^{-1} , \quad \hat{\mathbf{S}}_{n'l}^+ = \left(\hat{S} - \hat{\mu}^{(n')} \hat{S} \hat{\nu}^{(l)} \right)^{-1} .$$

Requiring that the transfer matrix reproduces the relations between $\psi_{n'}$ and ψ_l in the two solutions, one gets the following result

$$\hat{\mathcal{M}}_{n' \leftarrow l} = \langle l | \hat{\mathbf{S}}_{n'l}^+ | n' \rangle^{-1} \begin{pmatrix} A & B \\ -C & 1 \end{pmatrix} \quad (\text{E1})$$

where

$$\begin{aligned} A &= \langle n' | \hat{\mathbf{S}}_{n'l} | l \rangle \langle l | \hat{\mathbf{S}}_{n'l}^+ | n' \rangle - \langle l | \hat{S}^\dagger \hat{\mu}^{(n')} \hat{\mathbf{S}}_{n'l} | l \rangle \langle n' | \hat{S} \hat{\nu}^{(l)} \hat{\mathbf{S}}_{n'l}^+ | n' \rangle , \\ B &= \langle n' | \hat{S} \hat{\nu}^{(l)} \hat{\mathbf{S}}_{n'l}^+ | n' \rangle , \quad C = \langle l | \hat{S}^\dagger \hat{\mu}^{(n')} \hat{\mathbf{S}}_{n'l} | l \rangle . \end{aligned}$$

The determinant of the transfer matrix is

$$\text{Det} \left\| \hat{\mathcal{M}}_{n' \leftarrow l} \right\| = \frac{\langle n' | \hat{\mathcal{S}}_{n'l} | l \rangle}{\langle l | \hat{\mathcal{S}}_{n'l}^+ | n' \rangle}$$

The inverse matrix reads

$$\hat{\mathcal{M}}_{n' \leftarrow l}^{-1} = \langle n' | \hat{\mathcal{S}}_{n'l} | l \rangle^{-1} \begin{pmatrix} 1 & -B \\ C & A \end{pmatrix} \quad (\text{E2})$$

Applying the matching conditions for the conjugated waves $\bar{\psi}$ in Eq.(3.3), one can check that the the corresponding transfer matrix is given by the inverse of that for ψ *i.e.*

$$\bar{\psi}_{n'} = \bar{\psi}_l \hat{\mathcal{M}}_{n' \leftarrow l}^{-1}$$

Since $\bar{\psi}_{n'}^{(1)} \psi_{n'}^{(2)} = \bar{\psi}_l^{(1)} \hat{\mathcal{M}}_{n' \leftarrow l}^{-1} \hat{\mathcal{M}}_{n' \leftarrow l} \psi_l^{(2)} = \bar{\psi}_l^{(1)} \psi_l^{(2)}$, the conservation law in Eq.(2.9) is not affected by knots.

a. Transfer matrix 2×2 case

The transfer matrix for the case when the knot mixes 2 in- to 2 out-trajectories, can be obtained from the general expression in Eq.(E1). Algebraic simplifications of rather awkward expression gives a pretty compact result. Here, an alternative derivation, algebraically more transparent, is presented.

Call the trajectories of interest by 1 and 1', and consider calculation of $\hat{\mathcal{M}}_{1' \leftarrow 1}$ for given $\mu_{2'}$ and ν_2 in Eq.(C1). First note superconductivity influences the transfer matrix only via the trajectories 2 and 2'. Note also that in the normal metal case when $\mu_{2'} = \nu_2 = 0$, the transfer matrix is simply

$$\hat{\mathcal{M}}_{1' \leftarrow 1}^{(0)} = \begin{pmatrix} s & 0 \\ 0 & \frac{1}{s^*} \end{pmatrix} = s \begin{pmatrix} 1 & 0 \\ 0 & 0 \end{pmatrix} + \frac{1}{s^*} \begin{pmatrix} 0 & 0 \\ 0 & 1 \end{pmatrix} \quad (\text{E3})$$

where $s = S_{1'1}$.

Since the S -matrix is a electron-hole scalar, Eq.(3.1) is invariant relative to rotations in the electron-hole space. $\hat{\psi} \rightarrow \hat{\psi}_{\mathcal{O}} = \hat{\mathcal{O}}\psi$, and one can resolve the matching conditions in arbitrary basis.

The rotation

$$\hat{\mathcal{O}} = \frac{1}{1 - \mu_{2'} \nu_2} \begin{pmatrix} 1 & -\nu_2 \\ -\mu_{2'} & 1 \end{pmatrix}, \quad \hat{\mathcal{O}}^{-1} = \begin{pmatrix} 1 & \nu_2 \\ \mu_{2'} & 1 \end{pmatrix}$$

transforms $\begin{pmatrix} 1 \\ \mu_{2'} \end{pmatrix}$ to $\begin{pmatrix} 1 \\ \mu_{2'} \end{pmatrix}_{\mathcal{O}} = \begin{pmatrix} 1 \\ 0 \end{pmatrix}$ and $\begin{pmatrix} \nu_2 \\ 1 \end{pmatrix}$ to $\begin{pmatrix} 0 \\ 1 \end{pmatrix}$ as if in the normal state. Therefore, after the rotation, the transfer matrix is given by Eq.(E3), whereas in the original picture

$$\hat{\mathcal{M}}_{1' \leftarrow 1} = \hat{\mathcal{O}}^{-1} \hat{\mathcal{M}}_{1' \leftarrow 1}^{(0)} \hat{\mathcal{O}}.$$

Inserting Eq.(E3), the transfer matrix reads

$$\hat{\mathcal{M}}_{1' \leftarrow 1} = \frac{1}{1 - \mu_{2'} \nu_2} \left(s \begin{pmatrix} 1 \\ \mu_{2'} \end{pmatrix} (1, -\nu_2) - \frac{1}{s^*} \begin{pmatrix} \nu_2 \\ 1 \end{pmatrix} (\mu_{2'}, -1) \right). \quad (\text{E4})$$

One recognizes the combinations entering \hat{g}_\pm^R in Eq.(2.17) with the important difference that ν_2 and $\mu_{2'}$ are parameters of the wave functions not at the same point but across the knot.

Finally,

$$\hat{\mathcal{M}}_{1' \leftarrow 1} = \frac{1+S}{2s*} \left(1 - \frac{R}{1+S} \hat{g}_{2' \bullet 2} \right) \quad (\text{E5})$$

where $S = |s|^2$, $R = 1 - S$, and

$$\hat{g}_{2' \bullet 2} = \frac{1}{1 - \mu_{2'} \nu_2} \begin{pmatrix} 1 + \mu_{2'} \nu_2 & -2\nu_2 \\ 2\mu_{2'} & -1 - \mu_{2'} \nu_2 \end{pmatrix}$$

is normalized $\hat{g}_{2' \bullet 2}^2 = 1$, “across-the-knot” Green function. It can be presented in a factorized form as follows

$$\frac{1}{2} (1 + \hat{g}_{2' \bullet 2}) = \frac{1}{1 - \mu_{2'} \nu_2} \begin{pmatrix} 1 \\ \mu_{2'} \end{pmatrix} (1, -\nu_2) \quad (\text{E6})$$

Up to normalization, $\begin{pmatrix} 1 \\ \mu_{2'} \end{pmatrix} = \phi_+^{(2')}$ where $\phi_+^{(2')}$ is the knot value of ϕ_+ on the trajectory $2'$, and $(1, -\nu_2) = \bar{\phi}_-^{(1)}$. Taking into consideration Eqs.(2.14), and (2.21), one concludes from Eq.(E6) that $(1 + \hat{g}_{2' \bullet 2}) \propto (1 + \hat{g}_{2'}) (1 + \hat{g}_2)$ so that

$$(1 + \hat{g}_{2' \bullet 2}) = \mathcal{N}^{-1} (1 + \hat{g}_{2'}) (1 + \hat{g}_2) \quad , \quad \mathcal{N} = \frac{1}{2} \text{Sp} (1 + \hat{g}_{2'}) (1 + \hat{g}_2) \quad , \quad (\text{E7})$$

where the normalization $\frac{1}{2} \text{Sp} (1 + \hat{g}_{2' \bullet 2}) = 1$ fixes the proportionality coefficient \mathcal{N} . This formula expresses the “across-the-knot” function via Green’s function on the trajectories 2 and $2'$.

After some algebra, one gets another form of Eq.(E7):

$$\hat{g}_{2' \bullet 2} = \frac{1}{1 + \frac{1}{2} [\hat{g}_{2'}, \hat{g}_2]_+} \left(\hat{g}_{2'} + \hat{g}_2 + \frac{1}{2} [\hat{g}_{2'}, \hat{g}_2]_- \right) \quad .$$

(The anticommutator $\frac{1}{2} [\hat{g}_{2'}, \hat{g}_2]_+$ in the denominator is proportional to the unit matrix and does not pose any problem).

REFERENCES

* Also at A. F. Ioffe Physico-Technical Institute, 194021 St.Petersburg, Russia.

- [1] G. Eilenberger, Z.Phys., **214**, 195, (1968).
- [2] A.I. Larkin and Yu.N. Ovchinnikov, Zh. Eksp. Teor. Fiz. **55**, 2262 (1968) [Sov. Phys.-JETP, **28**, 1200 (1969)] A.I. Larkin and Yu.N. Ovchinnikov, in *Nonequilibrium Superconductivity*, edited by D.N. Langenberg and A.I. Larkin, (Elsevier, Amsterdam, 1984);
- [3] A. Schmid in *Nonequilibrium Superconductivity*, edited by K.E. Gray (Plenum, N.Y., 1981);
- [4] J.W. Serene, and D. Rainer, Phys. Rep., **4**,221, (1983).
- [5] W. Belzig, F. K. Wilhelm, C. Bruder, G. Schön, and A. D.Zaikin, *Quasiclassical Green's function approach to mesoscopic superconductivity*, cond-mat/9812297.
- [6] A.V. Zaitsev, Zh. Eksp. Teor. Fiz. **86**, 1742 (1984) [Sov. Phys. JETP **59**, 1015 (1984)].
- [7] M. Ashida, S. Aoyama, J. Hara, and K. Nagai, Phys. Rev. **B40**,8673 (1989) Y. Nagato, K. Nagai and J. Hara, J. Low Temp. Phys. **93**, 33 (1993); S. Higashitani and K. Nagai, J. Phys. Soc. Japan. **64**, (1995); Y. Nagato and K. Nagai, Phys. Rev. **B** **51**, 16254 (1995); Y. Nagato, M. Yamamoto and K. Nagai, J. Low. Temp. Phys. **110**, 1135 (1998);
- [8] Y. Nagato, S. Higashitani, K. Yamada and K. Nagai, J. Low. Temp. Phys. **103**, 1 (1996); K. Yamada, Y. Nagato, S. Higashitani and K. Nagai, J. Phys. Soc. Jpn. **65**, 1540 (1996); K. Nagai, in *Quasiclassical theory of superconductivity*, ed. D. Rainer and J.A. Sauls, p. 198 (1998).
- [9] S.-K. Yip, J. Low Temp. Phys. **109**, 547 (1997).
- [10] P. G. de Gennes, *Superconductivity of Metals and Alloys*, (Addison-Wesley Publishing Co., 1989).
- [11] A.L. Shelankov, Zh. Eksp. Teor. Fiz. **78**, 2359 (1980), Sov. Phys. JETP **51**, 1186 (1980).
- [12] It follows from Eq.(1.2), that $\psi_e(\mathbf{r}, t|\{\mathbf{A}\})$ and $\psi_h^*(\mathbf{r}, t|\{\mathbf{A}\})$ satisfy same equation. Thus, $\psi_e(\mathbf{r}, t) = \psi_h^*(\mathbf{r}, t)$ provided $\psi_e(\mathbf{r}, 0) = \psi_h^*(\mathbf{r}, 0)$.
- [13] Taking the Larmor orbits as an example, the electron and hole circle in the *same* direction, clock- or anti-clockwise. However, their trajectories are not the same: From Eq.(1.4) one can see that the Larmor circle centre positions $\mathbf{R}_L^{(e,h)}$ for the electron and hole, created at $t = 0$ at the same $\mathbf{r}_0 - \mathbf{p}_0$ point, are different $(\mathbf{R}_L^{(e)} - \mathbf{r}_0) \cdot \mathbf{p}_0 = -(\mathbf{R}_L^{(h)} - \mathbf{r}_0) \cdot \mathbf{p}_0$.
- [14] Suppose that the trajectory without magnetic field is a straight line in the x -direction. In a weak magnetic field $\mathbf{B} \parallel \hat{z}$ the Lorentz force transforms the straight line into the parabola $y(e, h) = \pm x^2/2R_c$ in the $x - y$ plane; here $+(-)$ refers to electron (hole) and $R_c = v/\omega_c$, $\omega_c = |eB/mc|$ being the cyclotron frequency. The broadening $w(x)$ of a packet where both the electron and hole component are present, is of order of $w(x) \sim |y(e) - y(h)| \sim x^2/R_c$. The packet acquires the transverse width $w \sim \xi^2/2R_c$ when the characteristic time $\sim \hbar/\Delta$ has elapsed and $x \sim \xi$. The broadening should be compared with the typical spatial resolution required in the theory *i.e.* the coherence length ξ . Then, a dimensionless characteristic of the broadening is $\frac{\xi}{w(\xi)} \sim \frac{\xi}{R_c} \sim \frac{\omega_c}{\Delta}$.
- [15] N.B. Kopnin, Phys. Rev. **B** **54**, 9475 (1996).
- [16] L.P. Gor'kov and J.R. Schrieffer, Phys. Rev. Lett. **80**, 3360 (1980).
- [17] A.F. Andreev, Zh.Eksp.Teor.Fiz., **46**, 1823 (1964) [Sov.Phys. JETP, **19**, 1288, (1964)].

[18] Generally speaking $\nabla U \neq 0$ and the trajectory may be different from a straight line. Then, one introduces the envelope ψ by the anzats $\Psi(\mathbf{r}, t) = \psi(r) e^{\frac{i}{\hbar} S(\mathbf{r})} e^{\frac{i}{\hbar} Et}$ where $S(\mathbf{r})$ is the classical action. One gets the Andreev equation again where $\mathbf{v} \cdot \nabla$ has the meaning of the derivative with respect to the coordinate along the trajectory.

[19] It is important to realize that the knot couples together all four directions. Unlike usual scattering theory where the in-coming channels 1 and 2 in Fig.1 would be independent, in superconductors one must include all the channels coupled by scattering. The formal difference arises due to the two-component character of the wave functions. In physical terms, the arrows show the direction of the momentum rather than velocity; apart the momentum, the latter depends also on the character of an excitation, electron or hole. On the knot, an electron-like excitation coming along 1 may be converted into a hole which goes away along nominally in-coming trajectory 2.

[20] A.L. Shelankov, Pis'ma Zh. Eksp. Teor. Fiz. **32**, 122 (1980) [JETP Lett. **32**, 111 (1980)].

[21] T. Kotlos, and U. Smilansky, Phys. Rev. Lett. **79**, 4794 (1997).

[22] A.L. Shelankov, Thesis, the Ioffe Physico-Technical Institute, Leningrad, 1980.

[23] A.L. Shelankov, J. Low Temp. Phys., **60**, 29, 1985.

[24] N. Schopol, and K. Maki, Phys. Rev. **B 52**, 490 (1995).

[25] N. Schopol “*Transformation of the Eilenberger Equations of Superconductivity to a Scalar Riccati Equation*”, cond-mat/9804064 and in *Quasiclassical theory of superconductivity*, ed. D. Rainer and J.A. Sauls, p. 88 (1998).

[26] A. L. Fauchere, W. Belzig, G. Blatter, Phys. Rev. Lett. **82**, 3336 (1999) (cond-mat/9901112).

[27] A.V. Svidzinskii, and V.A. Slusarev, Phys. Lett., **272**, 22 (1968); A.V. Svidzinskii, *Spatially Inhomogeneous Problems in the Theory of Superconductivity*, Nauka, M., 1982, (in Russian).

[28] L. P. Gorkov, N.B. Kopnin Zh. Eksp. Teor. Fiz. **64**, 360 (1973).

[29] The phase of the exponents in Eq.(2.1) is the free motion classical action. If the particle is subject to a smooth time-reversal symmetry conserving potential, it can be easily incorporated into the scheme. In this case the trajectory is found from the classical equation of motion.

[30] More generally, the matrix \hat{H}^R has the contribution $(-\Phi)\hat{1}$ where $\Phi = e\varphi + \dot{\chi}/2$ is the gauge invariant potential made of the scalar potential φ and the phase of the order parameter χ . The substitution $g \rightarrow \exp\left(i \pm \int_{x_1}^{x_2} dx \Phi(x)\right) \hat{g}(x_1, x_2)$ eliminates Φ from the equations.

[31] Obvious properties of the “formating” operation: (i) $\mathcal{F}_R[\hat{X} + \lambda\hat{1}] = \mathcal{F}_R[\hat{X}]$; (ii) $\mathcal{F}_R[\lambda\hat{X}] = \mathcal{F}_R[\hat{X}]$.

[32] The knot assumed to be “irreducible” *i.e.* the channels can not be combined in disconnected groups with the number of channels less than N .

[33] Note that the amplitude of the Andreev reflection by the knot, B_l , is a real function of a 's and b 's, *i.e.* the coefficients in the expansion of B_l in series of $a_i^n b_f^m$, which are combinations of the S-matrix elements, are real.

[34] M. Fogelström, D. Rainer, and J.A. Sauls, Phys. Rev. Lett. **79**, 281 (1997).

[35] A.L. Shelankov, Sov. Phys. Solid State **26**, 981 (1984); *ibid* **27**, 965 (1985).

[36] P. Visani, A.C. Mota, and A. Polini, Phys. Rev. Lett. **65**, 1514 (1990); A.C. Mota, P.

Visani, A. Polini, and K. Auple, Physica B **197**, 95, (1994).
[37] M. Eschrig, Los-Alamos e-print archive, cond-mat/9907312.

FIGURES

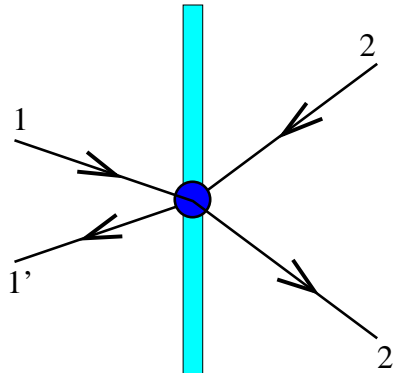


FIG. 1. Scattering on a partially transparent specular interface. The interface is depicted as the shaded region. The arrows show the direction of the (electron) velocity. The in-coming (out-going) trajectories are denoted 1 and 2 (1' and 2'). The filled circle, the knot (see text), is the “black box” where the scattering occurs.

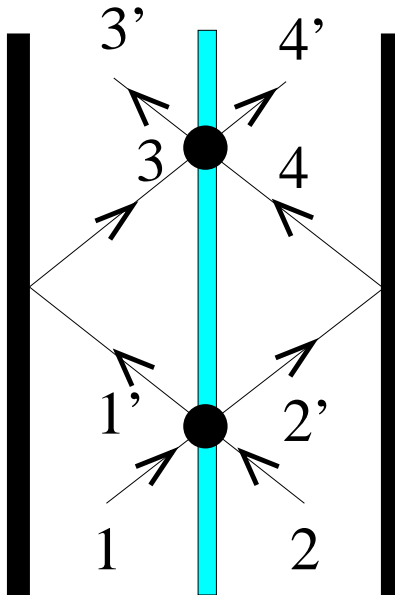


FIG. 2. The typical trajectory in an ideal sandwich with the layers of an equal thickness and parallel surfaces.

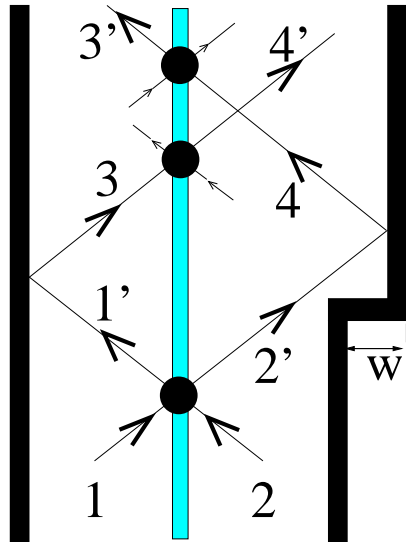


FIG. 3. The typical trajectory in a sandwich with a rough surface. The roughness is shown schematically as a step, W being the height of the step. Unlike the ideal case in Fig. 2, the paths 1' and 2' return to the interface at different points.

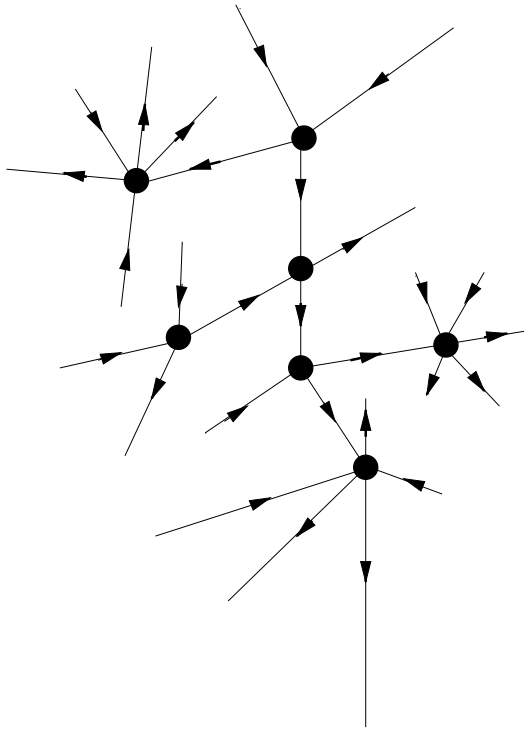


FIG. 4. An example of a tree-like trajectory. Pieces of the straight lines show the trajectories before or after they enter a knot (filled circles), *i.e.* before or after a collision with an interface. There is only one path connecting any two points on the tree so that the tree is effectively 1-dimensional.

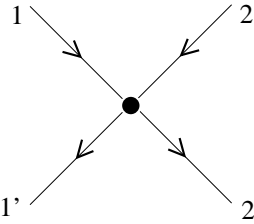


FIG. 5. Simplest 2×2 knot with two incoming 1 and 2, and two outgoing channels $1'$ and $2'$ (schematically).

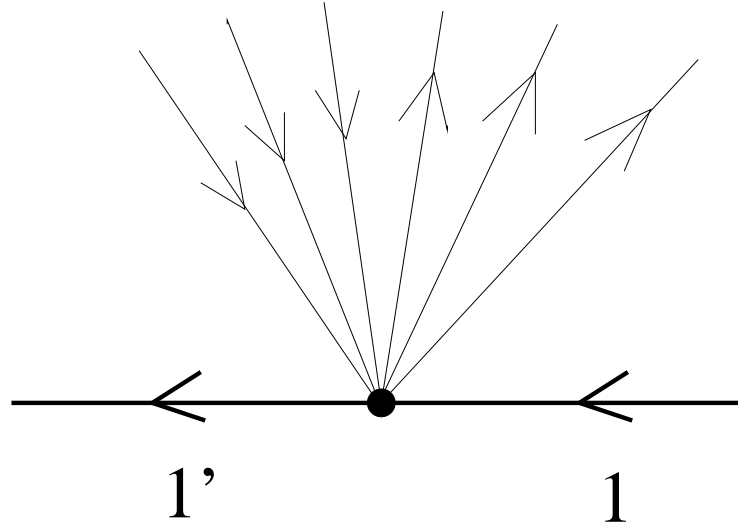


FIG. 6. For a many channel knot, one chooses a pair of trajectories, one in- and one out- (denoting them 1 and $1'$), and considers them as a single trajectory with a knot on it. The transfer matrix relates to each other the wave functions across the knot.

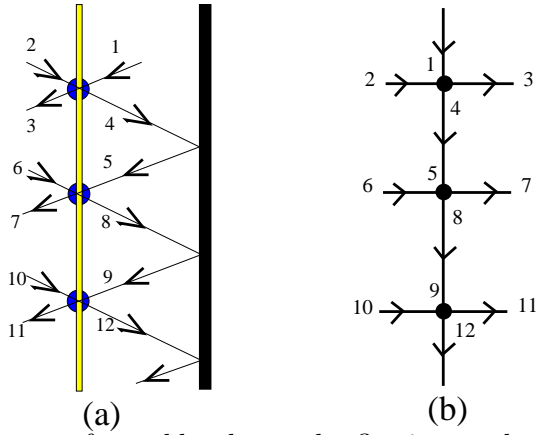


FIG. 7. The typical trajectory formed by the total reflection on the outer surface and the partial reflection/transmissions on the interface (a). The numbers serve as markers for both direction and position. In (b), the structure of the tree-like trajectory is shown with the numbering as in (a).

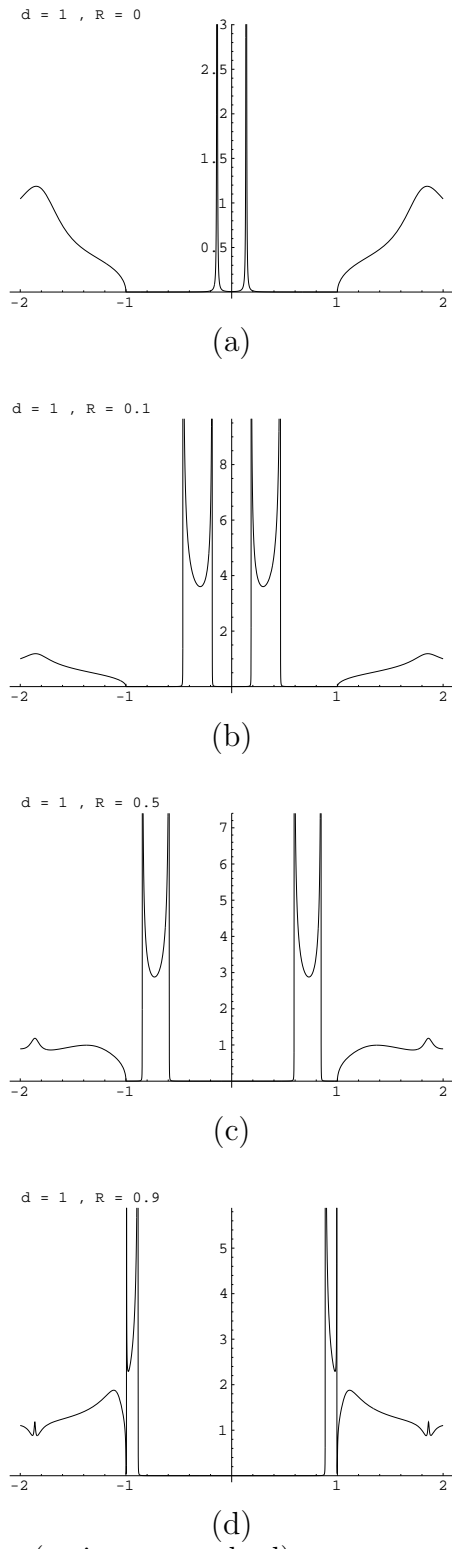


FIG. 8. The density of states (trajectory resolved) versus energy ε/Δ at the interface of a bulk superconductor with the pair potential Δ_l and a film $\Delta_r = -\Delta_l$ (see Fig. 7). The film thickness d is measured along the trajectory in units $v/\|\Delta\|$. The interface reflectivity $R = 0, 0.1, 0.5, 0.9$ in (a,b,c,d) respectively.

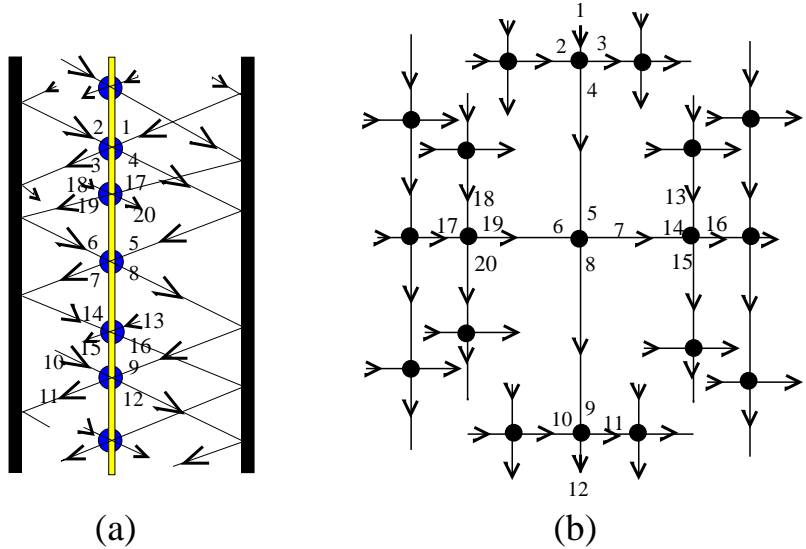


FIG. 9. (a) Real space classical trajectories of a particle in a two layers system formed by multiple reflections on the outer surface and the interface between layers. Numbers tag both the position of the particle on the trajectory as well as the direction. (b) The structure of the tree-like trajectory is shown. The points in real space and on the tree are marked by the same numbers in (a) and (b).

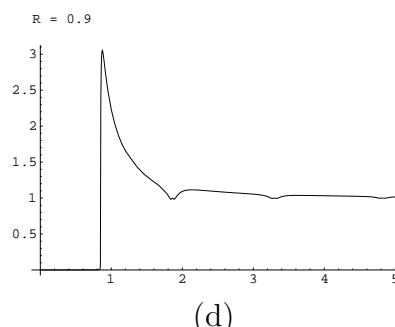
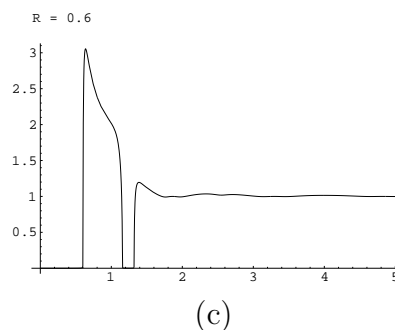
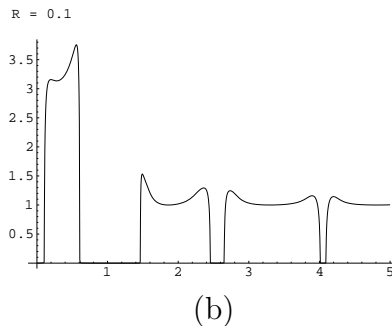
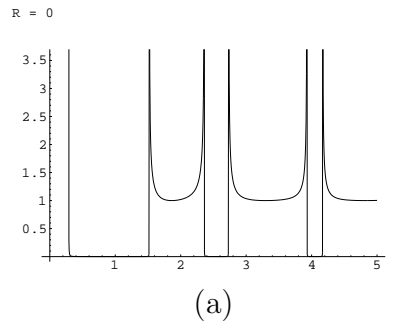


FIG. 10. Trajectory resolved density of states versus energy ε/Δ at the interface. The order parameter $\Delta_l = -\Delta_r$. The thickness of the both layers is $v/|\Delta_l|$. The reflection R , shown at the top of the pictures, is 0, 0.1, 0.6, and 0.9 in (a), (b), (c), and (d), respectively.

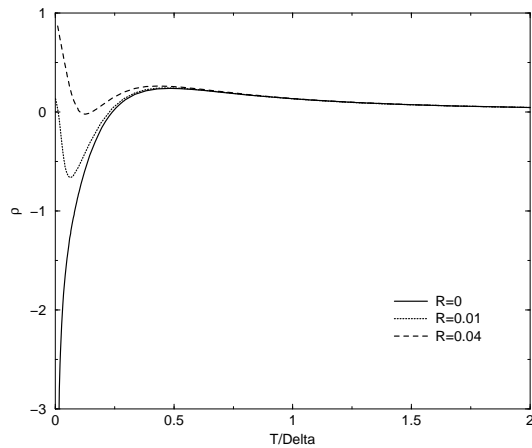


FIG. 11. The effective superfluid density of a system of two layers, l and r , of equal thickness $d_l = d_r = v/|\Delta_l|$ with the π phase difference $\Delta_l = -\Delta_r$ for different reflectivity of the interface $R = 0, 0.01, 0.04$